

TRAINING LANGUAGE MODELS TO EXPLAIN THEIR OWN COMPUTATIONS

Belinda Z. Li^{1,2*}, Zifan Carl Guo², Vincent Huang¹, Jacob Steinhardt¹, Jacob Andreas^{1,2}

¹Transluce ²MIT CSAIL

ABSTRACT

Can language models (LMs) learn to faithfully describe their internal computations? Are they better able to describe themselves than other models? We study the extent to which LMs’ privileged access to their own internals can be leveraged to produce new techniques for explaining their behavior. Using existing interpretability techniques as a source of ground truth, we fine-tune LMs to generate natural language descriptions of (1) the information encoded by LM features, (2) the causal structure of LMs’ internal activations, and (3) the influence of specific input tokens on LM outputs. When trained with only tens of thousands of example explanations, explainer models exhibit non-trivial generalization to new queries. This generalization appears partly attributable to explainer models’ privileged access to their own internals: using a model to explain its own computations generally works better than using a *different* model to explain its computations (even if the other model is significantly more capable). Our results suggest not only that LMs can learn to reliably explain their internal computations, but that such explanations offer a scalable complement to existing interpretability methods.¹

1 INTRODUCTION

When language models (LMs) are prompted to explain decisions—to describe what features they relied on, or what intermediate computations they performed when generating an answer—their outputs are often plausible (Korbak et al., 2025). But even when plausible, these explanations may not have any relationship to the internal computation that gave rise to LMs’ decisions in the first place. Indeed, work using attribution, feature visualization, and mechanistic interpretability techniques (Simonyan et al., 2013; Covert et al., 2020; Templeton et al., 2024) has shown that LMs’ verbalized explanations sometimes systematically fail to describe the factors that determine their decisions (Turpin et al., 2023; Chen et al., 2025; Barez et al., 2025).

Can we fix this problem, and train LMs so that their verbalized explanations faithfully describe their internal computations? Several recent papers (Binder et al., 2025; Song et al., 2025b; Plunkett et al., 2025) have studied the related question of whether models can describe features of their own *output distributions*, arguing that models might be able to leverage **privileged access** to their own internals to do so effectively. In this paper, we are interested in an even deeper form of privileged access: whether models can learn to describe not only their outputs, but their *internal* representations and mechanisms, and whether privileged self-access enables them to do so better than learned explanation-generating methods derived from other models. We state our main hypothesis as follows:

The Privileged Access Hypothesis

Models trained to explain their own internal computations can do so more accurately than other models trained to explain them.

*Correspondence to Belinda Z. Li <bzl@mit.edu>.

¹Code and data at <https://github.com/TransluceAI/introspective-interp>.

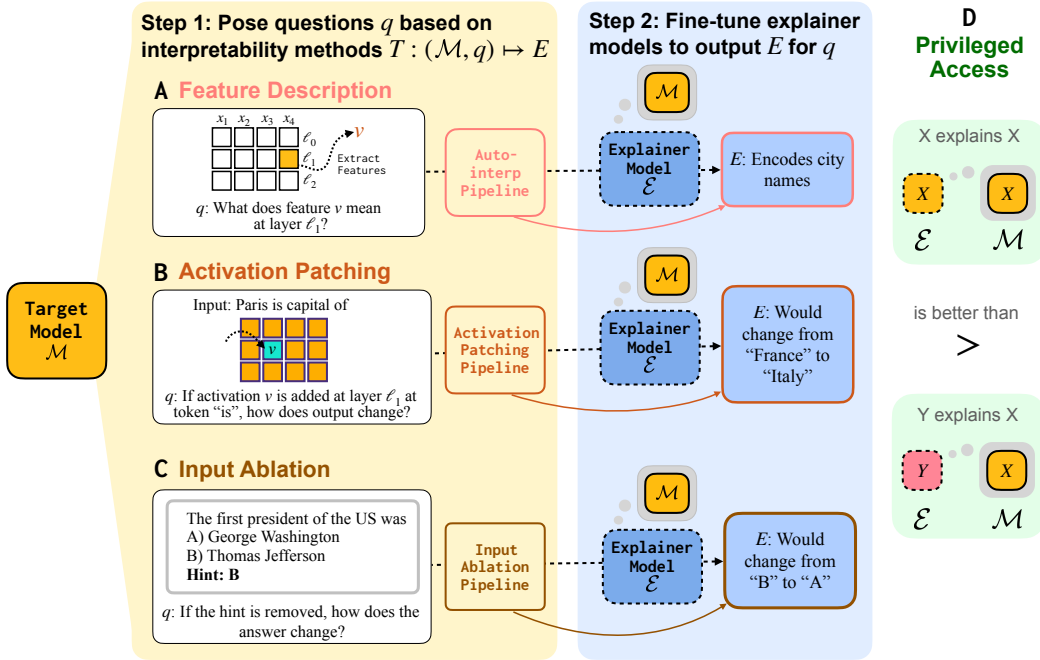


Figure 1: Overview of our methods for training models to describe their own internal procedures. As a first step, we extract answers to three types of question about the target model using different interpretability methods: (A) descriptions of features of the target model’s hidden representations via an auto-interp procedure, (B) explanations about what parts of the model affect the output via activation patching, (C) explanations about what parts of the input affect the output via input ablation. As a second step, we fine-tune three explainer models to produce each of the three types of explanations. (D) After fine-tuning various explainer models on various target models, we find evidence of privileged access for all three explanation types, and use this to obtain data-efficient explainers.

To explore this hypothesis, we fine-tune various *explainer* models to predict three aspects of *target* models’ internal procedures:²

1. Descriptions of internal features, specifically the kinds of inputs that activate them (**feature descriptions**; Figure 1A).
2. Outcomes of interventions to internal activations (**activation patching**; Figure 1B).
3. Descriptions of decision rules, specifically the important tokens for a decision (**input ablation**; Figure 1C). We focus on a setting where recent work found that reasoning models failed to produce faithful chains-of-thought (Chen et al., 2025), in order to explore whether training can improve faithfulness. This setting also bears similarities to Binder et al. (2025) due to measuring self-access to the model’s output distributions.

Our main experiments focus on feature descriptions, where we find evidence of privileged access—our target model is better explained by itself than by other explainer models, even when the other model is generally more capable (e.g. larger or instruction-tuned).

We dive deeper into this phenomenon and probe the generality of this hypothesis, finding that:

1. **LMs can be fine-tuned to self-explain:** As in past work (Li et al., 2025), we find that explanation capabilities are not always natively present in models, and must be acquired

²This paper treats the *target model* as fixed and only fine-tunes the *explainer model*. While this setup does not constitute *self-explanation* in the strictest sense (since the explainer’s output distribution changes), we believe it is more useful to explain pre-trained models than enforce this strict notion of self-consistency. We discuss the implications of this simplification in Section 7. For the rest of this paper, we use the term “self-explaining” in this looser sense.

via fine-tuning. A small amount of fine-tuning enables LMs to faithfully describe their internal features, significantly outperforming zero-shot methods (Kharlapenko et al., 2024; Chen et al., 2024a) and nearest-neighbor SAE features (Huben et al., 2024). Furthermore, a model’s ability to explain (its own or others’) features is correlated with the degree of similarity between the explainer and target models (§3.4).

2. **Self-explaining is data-efficient:** Self-explaining is approximately a hundred times more sample-efficient than a nearest neighbors baseline, achieving comparable results with only 0.8% of the training data (§4). This makes self-explaining a scalable approach to generating feature descriptions.
3. **Privileged access extends to other tasks:** we train models to explain the effects of activation patching (§5.1) and input ablation (§5.2). For the first task, we see the same pattern of privileged access as in feature descriptions. For the second, we see a slightly different pattern, as some models appear to be universally stronger explainers (e.g. Qwen outperforms Llama across the board); however, we still observe evidence of privileged access here (e.g. Qwen is better at explaining itself than explaining Llama, and vice versa).

Taken together, these results suggest that even when language models cannot faithfully self-explain as a result of ordinary training, they can learn to do so through an objective that enforces consistency between their external explanations and their internal procedures. This reframes interpretation as not only an external analysis problem, but as a capability that can be trained into LMs themselves; by leveraging privileged access to internal computations, “introspective interpretability” techniques offer an avenue towards scalable understanding of model behavior.

2 METHODS

In this section we describe a general framework for training models to verbalize different aspects of their internal states, and then instantiate it with three specific explanation types.

2.1 DEFINITIONS AND TASK

Abstractly, a neural **model** \mathcal{M} can be represented as a pipeline $x \rightarrow h \rightarrow y$ that maps **inputs** x to **hidden representations** h to **outputs** y . An **explanation** E of the neural network may enable us to answer **questions** q about what information in x is represented in h , how that information influences y , and what pieces of the model are responsible for each step.

For example, we may wish to answer a question $q = \textit{What inputs activate direction } v \textit{ at layer } l?$ If v activates highly on tokens *Tokyo*, *NYC*, and *Paris*, then an appropriate explanation E might be *city names*. We are interested in whether LMs can learn to generate them directly.

In this paper, we will train **explainer models** \mathcal{E} to produce explanations E for various **target models** \mathcal{M} and types of questions q . Abstractly, let $T : (\mathcal{M}, q) \mapsto E$ be a (model-external) **explanation procedure** that generates an explanation E answering a question q about model \mathcal{M} . We use T as supervision to train an explainer model, by minimizing the cross-entropy loss on the explanation:

$$\mathcal{L}_{\mathcal{E}} = -\mathbb{E}_q [\log p_{\mathcal{E}}(E = T(\mathcal{M}, q) \mid q)]. \tag{1}$$

Our experiments focus on explaining Transformer language models \mathcal{M} (Grattafiori et al., 2024; Yang et al., 2025), which consist of layers ℓ each containing attention and MLP blocks, and *residual stream* representations h_{ℓ} in between each layer. We also use Transformer language models as explainers \mathcal{E} . Throughout this paper, we use notation $x = (x_1, \dots, x_n)$ to refer to an input sequence with token positions $t \in [n]$. We use $h_{(\ell,t)}(x)$ to denote the residual stream activation of \mathcal{M} at layer ℓ and token position t for input x .

We will train explainer LMs to answer three types of questions q , described below.

2.2 FEATURE DESCRIPTIONS: WHAT DOES A MODEL-INTERNAL FEATURE REPRESENT?

Question q . For feature description, the question q is *what types of inputs activate direction v in the residual stream at layer l ?*

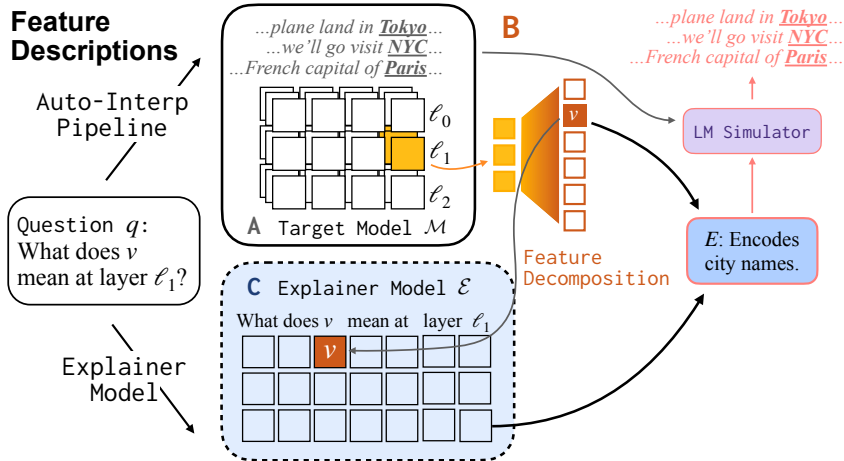


Figure 2: Training an explainer to predict **feature descriptions**. (A) We run a target model \mathcal{M} across many input contexts. (B) We then observe vectors v at layers ℓ and select an explanation E that best describes the contexts in which v is active, which we assess via a LM simulator. (C) Finally, we train an explainer model to respond with E when given the question q about what v means at layer ℓ , and find that it performs well on both held-out and OOD vectors v .

Interpretability procedure T . We make use of existing automated interpretability methods (Hernandez et al., 2022; Bills et al., 2023; Choi et al., 2024), which generate natural-language descriptions E by summarizing input tokens on which a given v is highly active.

Formally, let $a_v(x, \ell, t) = \langle h_{\ell, t}(x), v \rangle$ denote the activation of v in the residual stream representation of the token x_t . To obtain feature descriptions, we begin by prompting (or training) a “simulator” language model (LM simulator in Figure 2) to map from candidate descriptions E (e.g. *Encodes city names* in Figure 2) and input sequences x (e.g. *we’ll go visit NYC*) to predicted activations $\hat{a}(x, t, E)$ (e.g. outputting *0.1* for *visit* and *0.9* for *NYC*). See Figure 2B. We train the simulator following Choi et al. (2024) on FineWeb exemplars (Penedo et al., 2024) with Neuronpedia SAE labels.

Given the simulator, for each direction v , we search for the explanation E that maximizes correlation between simulated and true activations over all input data:

$$T_{\text{feat}}(\mathcal{M}, v, \ell) = \arg \max_E \mathbb{E}_x [\text{corr}_t(a_v(x, \ell, t), \hat{a}(x, t, E))] . \quad (2)$$

Intuitively, this procedure will assign each feature v an explanation E that describes the tokens on which v is most active. The prompts we use to encode q and E are given in Appendix D.

Training the explainer. \mathcal{E} receives a question q that contains a feature v and a layer ℓ , and is trained to generate the explanation E of when v is highly active at layer ℓ . We take v from the target model \mathcal{M} at its layer- ℓ residual stream, and pass it as a continuous token to the explainer, inserted at the embedding layer. This enables the explainer to accept arbitrary vectors v .³ See Figure 2C.

For explainer models whose hidden dimension does not match the target model, we introduce a **linear projection** $\Pi_\ell \in \mathbb{R}^{d_\mathcal{E} \times d_\mathcal{M}}$ from the target model hidden size $d_\mathcal{M}$ to the explainer model hidden size $d_\mathcal{E}$, which is trained jointly with the rest of LM parameters. We learn a separate projection per layer ℓ of the target model. We train explainers and projections to optimize:

$$\mathcal{L}_{\text{feat}} = -\mathbb{E}_{v, \ell} [\log p_\mathcal{E}(E = T_{\text{feat}}(\mathcal{M}, v, \ell) \mid \Pi_\ell v, \ell)] \quad (3)$$

Choice of directions v . Because activations h tend to be highly polysemantic (Elhage et al., 2022), interpretation is often done on *decomposed* representations, which are commonly either individual neurons (so v is a one-hot vector; Bau et al., 2020) or Sparse Auto-Encoder (SAEs) features obtained

³In early experiments, we also investigated explaining features v from other components of the target model, but found that explainers struggled to reproduce these explanations. We hypothesize that we need to patch features into the same type of location (i.e. the embedding layer is part of the residual stream).

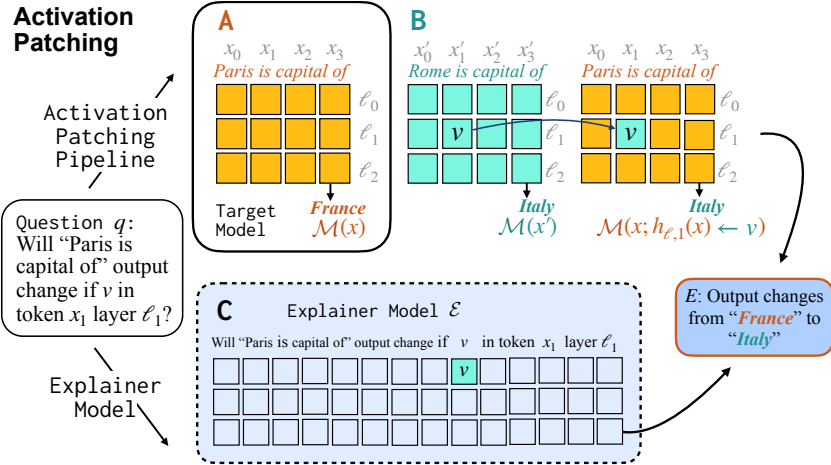


Figure 3: Training an explainer to predict **activation patching outcomes**. (A) We run a target model \mathcal{M} on an input x and obtain a prediction $\mathcal{M}(x)$. (B) We perform activation patching by running \mathcal{M} on a counterfactual input x' —in this example, patching in vector v from token x_1 and layer ℓ_1 of the counterfactual run into the original run—and then construct an explanation E about how the resulting prediction changes. (C) Finally, we train an explainer model to answer E when given a question q about the patching procedures.

from sparse dictionary learning approaches (with v being a member of the learned dictionary; Huben et al., 2024; Bricken et al., 2023). Our experiments train on SAE features, but test generalization to full activations and activation differences. See details in Section 3.2.

2.3 ACTIVATION PATCHING: WHAT INTERNAL COMPONENTS AFFECT THE PREDICTION?

Question q . For activation patching, we ask which hidden components are *causally important* for a model’s output (Meng et al., 2022; Zhang & Nanda, 2024). Specifically, the question q is on input x , (how) does changing the activation at layer ℓ and token x_t affect the output? An example is shown in Figure 3.

Interpretability Procedure T . We can answer questions of this form through activation patching and circuit tracing methods. Given an input x (*Paris is the capital of* in Figure 3), an activation patching experiment typically constructs an alternative input x' (*Rome is the capital of*). During the forward pass, we replace the activation $h_{\ell,t}(x)$ with the corresponding activation $h_{\ell,t}(x')$:

$$\mathcal{M}(x; h_{\ell,t}(x) \leftarrow h_{\ell,t}(x')) , \quad (4)$$

and we measure the change in the model’s output:

$$T_{\text{patch}}(\mathcal{M}, q) = T_{\text{patch}}(\mathcal{M}, x, \ell, t) = d(\mathcal{M}(x), \mathcal{M}(x; h_{\ell,t}(x) \leftarrow h_{\ell,t}(x'))), \quad (5)$$

where $d(\cdot, \cdot)$ is some measure of the difference between the two predictions. This process is illustrated in Figure 3B.

Training the explainer. Rather than directly predicting the numerical score in Equation (5), we train explainers \mathcal{E} to predict (1) *whether* the model output changes under patching, and (2) the *content* of the model output after patching. Similarly to Section 2.2, we insert v as a continuous token in the embedding layer of the explainer model. See Figure 3C.

Additionally, rather than patching activations one layer at a time, we modify representations at several layers simultaneously to ensure sufficient samples where the model’s output changed under intervention. We divide the target model’s layers into four blocks, and when performing activation patching, compute an aggregate representation $v = \text{avg}_{\ell_k} (h_{\ell_k,t}(x'))$ from the counterfactual input, then insert v at all corresponding layers of the original input.⁴ Finally, we optimize:

⁴We perform aggregation so that we only have to specify a single continuous token to the explainer.

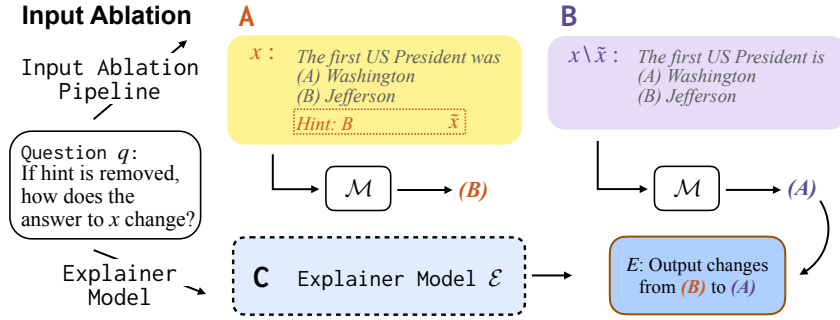


Figure 4: Training an explainer to predict **input ablation outcomes**. We run a target model \mathcal{M} on an input x (A), then identify whether a part of the input $\tilde{x} \subset x$ was important to the output by rerunning \mathcal{M} on $x \setminus \tilde{x}$ (B). Finally, we train an explainer model to answer question q about how the output changes when \tilde{x} is removed from x (C).

$$\mathcal{L}_{\text{patch}} = -\mathbb{E}_{x, x', t, \ell_{1 \dots i}} [\log p_{\mathcal{E}}(E = T_{\text{patch}}(\mathcal{M}, x, t, \ell_{1 \dots i}, v) \mid x, t, \ell_{1 \dots i}, v)] \quad (6)$$

The exact prompt and output templates are provided in Appendix D.

2.4 INPUT ABLATION: WHAT PARTS OF THE INPUT MATTER?

Question q . For input ablation, we ask which input tokens most influence the model’s prediction (Chang et al., 2025; Vafa et al., 2021). Specifically, the question q is *Are tokens \tilde{x} in x important to the model’s prediction?* For instance, in Figure 4, the question q asks whether the hint is important to the answer.

Interpretability Procedure T . As with activation patching, we can remove (subsets of) tokens in x and identify which ones cause predictions y to change. Let $\tilde{x} \subseteq x$ be a subset of tokens to remove. Input ablation measures how much the model output changes when we take an input x (e.g. *The first US president...* in Figure 4) and remove a subset of tokens \tilde{x} (e.g. *Hint: B*):

$$T_{\text{input}}(\mathcal{M}, x, \tilde{x}) = d(\mathcal{M}(x), \mathcal{M}(x \setminus \tilde{x})), \quad (7)$$

where d measures difference in the model’s outputs. This process is illustrated in Figure 4B.

Training the explainer. \mathcal{E} receives a question q that contains a multiple-choice reasoning question c with a hint \tilde{x} , and is asked to predict (1) whether removing \tilde{x} would change the model’s answer (the *has-changed* value), and (2) the new output without the hint (the *content* of the change). See Figure 4C. Formally, the objective we optimize is:

$$\mathcal{L}_{\text{input}} = -\mathbb{E}_{x, \tilde{x}} [\log p_{\mathcal{E}}(E = T_{\text{input}}(\mathcal{M}, x, \tilde{x}) \mid x, \tilde{x})] \quad (8)$$

Full prompt and output templates are provided in Appendix D.

3 PRIVILEGED ACCESS IMPROVES EXPLANATIONS

In this section, we (1) show that models can be fine-tuned to generate feature descriptions and generalize to new features and feature bases, and (2) provide evidence that this capability relies on privileged access. Our experiments focus on feature description (§2.2), where we train explainer models to verbalize descriptions of the target model’s features. We study additional tasks (patching, input ablation) in §5.

3.1 MODELS AND TRAINING DATA

We study Llama-3.1-8B (Grattafiori et al., 2024) as the target model, and test five different explainer models (Llama-3.1-8B, Llama-3-8B, Llama-3.1-8B-Instruct, Llama-3.1-70B, Qwen3-8B; Yang

et al., 2025).⁵ We select the explainer models that differ from the target model in attributes such as architecture (Qwen3-8B), size (Llama-3.1-70B), and training regimen (Llama-3.1-8B-Instruct), to investigate the effect of each of these factors. We fine-tune each model to be an effective explainer as described in Equation (3). For Llama-3.1-8B, we report results with both LoRA (Hu et al., 2022) and full-parameter fine-tuning, while for Llama-3.1-70B we only report LoRA due to compute constraints, and for other models we only report full-parameter fine-tuning.

For models that require projection layers Π_ℓ due to hidden-size mismatch (Qwen3-8B, Llama-3.1-70B), we *randomly initialize* those layers and train them with the rest of the parameters.⁶ We additionally train a version of Llama-3.1-70B where the projection layer is *pre-trained* to minimize $\|h_{\ell,t}^\mathcal{E} - \Pi_\ell \cdot h_{\ell,t}^\mathcal{M}\|_2$ on FineWeb samples (Penedo et al., 2024), or the distance between the the layer- ℓ , token- t explainer activation $h_{\ell,t}^\mathcal{E}$, and the projected target activation $\Pi_\ell \cdot h_{\ell,t}^\mathcal{M}$ from the same layer, token location.

To generate training data, we use Llama-Scope (He et al., 2024) to obtain residual stream SAE features for Llama-3.1-8B target models, which we use for the direction v . We use the Llama-3.1-8B-LXR-32x features, which maps the residual stream after each layer to 131K features (32 times larger than the residual hidden dimension).⁷ Ground-truth explanations E for each feature were obtained from Neuronpedia (Lin, 2023).

3.2 EVALUATION SET AND METRICS

We train on a subset of SAE features S_{train} , then evaluate generalization both in-distribution and out-of-distribution, on three types of features:

Held-out SAE features (SAE). We hold out a subset of 1550 SAE features (50 per layer) for testing.

Full Activations (ACT). We test out-of-distribution generalization to full residual stream activations $h_{(\ell,t)}(x)$ on inputs x sampled from FineWeb (Penedo et al., 2024).

Activation Differences (Δ ACT). Differences between counterfactual pairs of inputs allow us to isolate the effect of a single pointwise change. We create counterfactual pairs (x, x') from the Counterfact dataset (Meng et al., 2022) using the procedure described in Section 2.3 and extract activation differences $v = h_{\ell,t}(x) - h_{\ell,t}(x')$.

On each of these evaluation sets, we consider two types of metrics:

LM judge. For SAE features, gold descriptions are available, so we use an LM judge to assess the similarity of the predicted description to the gold description, on a scale of 0 (no similarity) to 1 (very similar), in increments of 0.25. We use GPT-4.1-mini as the judge; the exact prompt can be found in Section A.2. Human assessment of 200 samples of the LM judge results shows 81.25% human agreement.⁸

Simulator score. We also use *simulator score*, described in Equation (2), which measures the Pearson correlation between the model’s true activations and its predicted activations based on the explanation $\mathcal{E}(v)$ on each sample x .

3.3 BASELINES

To contextualize our results, we compare to two different baselines:

Nearest neighbors. To evaluate whether explainer models exhibit nontrivial generalization to unseen features, we compare to a nearest-neighbor baseline that, given a new feature or representation, finds the single most similar feature from the training set, and outputs its associated description. Let S_{train} denote the set of features used for training, and let $S_{train,\ell}$ denote the subset of SAE features at layer ℓ . We evaluate two nearest-neighbor baselines:

⁵Details can be found in Section A.1.

⁶For LoRA training, these layers are included in the set of parameters trained via low-rank updates.

⁷We run additional experiments with Gemma 2 (Gemma Team et al., 2024), whose data generation details can be found in Section B.1.

⁸Details of this assessment can be found in Section A.2.

Explainer	SAE		ACT	Δ ACT
	LM judge	Simulator	Simulator	Simulator
Llama-3.1-8B	76.2 \pm 0.9	45.1 \pm 0.7	49.7 \pm 0.6	32.0 \pm 0.8
Llama-3.1-8B (LoRA)	76.0 \pm 0.9	45.6 \pm 0.8	50.6 \pm 0.6	34.0 \pm 0.8
Llama-3-8B	77.0 \pm 0.9	44.6 \pm 0.7	49.3 \pm 0.6	32.4 \pm 0.7
Llama-3.1-8B-Instruct	77.1 \pm 0.8	42.7 \pm 0.7	46.9 \pm 0.7	29.9 \pm 0.7
Qwen3-8B	70.3 \pm 0.9	40.6 \pm 0.8	21.1 \pm 0.7	12.3 \pm 0.4
Llama-3.1-70B (LoRA)				
random projection	63.9 \pm 1.0	39.5 \pm 0.8	12.6 \pm 0.4	12.2 \pm 0.4
pre-trained proj.	74.1 \pm 0.9	45.2 \pm 0.7	33.8 \pm 0.7	20.6 \pm 0.6
NN-all	58.5 \pm 1.0	33.7 \pm 0.8	38.9 \pm 0.7	18.5 \pm 0.6
NN-layer	53.9 \pm 0.9	29.4 \pm 0.7	40.7 \pm 0.7	28.6 \pm 0.7
SelfIE Best of 5				
Llama-3.1-8B	40.1 \pm 1.0	36.4 \pm 0.8	43.3 \pm 0.6	21.0 \pm 0.6
Llama-3.1-8B-Instr.	40.4 \pm 0.9	36.4 \pm 0.8	43.5 \pm 0.7	20.1 \pm 0.6
Gold SAE labels	100 \pm 0.0	43.3 \pm 0.8	-	-

Table 1: **A target model’s features are best explained by itself and its variants.** We compare explainer methods on Llama-3.1-8B residual features, including trained models, nearest-neighbor baselines, untrained SelfIE variants, and gold SAE labels. Scores (mean \pm standard error) over two metrics (LM-judge, simulator scores) and three datasets—held-out SAE, FineWeb activations (ACT), and CounterFact differences (Δ ACT)—are reported, each scaled to 100. **Bold** indicates no significant difference from the best model (paired t -test, $p \geq 0.05$) for each metric. Trained Llama-3.1-8B and closely related models outperform other explainer methods—including gold SAE labels when scored via the simulator. Furthermore, **activation alignment improves explainer performance**: pre-training a projection layer to align features improves Llama-3.1-70B.

1. **Layerwise nearest neighbor.** We restrict retrieval to features from the same layer ℓ , so that the retriever explanation is $\mathcal{E}_{\text{NN-layer}}(v, \ell) = D(\arg \max_{v_i \in S_{\text{train}, \ell}} \langle v_i, v \rangle)$, where D is the function mapping training features to their explanations.
2. **All-layer nearest neighbor.** We retrieve from the training feature set across all layers: $\mathcal{E}_{\text{NN-all}}(v) = D(\arg \max_{v_i \in S_{\text{train}}} \langle v_i, v \rangle)$.

SelfIE. Following SelfIE (Chen et al., 2024a), we directly patch v into the embedding layer of a non-finetuned model,⁹ and prompt the LM to define the feature. We use standard prompts found to work well for self-explanations (Kharlapenko et al., 2024).¹⁰ Prior works have found that SelfIE is sensitive to the scale of v when it is inserted (Kharlapenko et al., 2024). We report results on the *best* explanation across 5 possible scales (v , $5v$, $10v$, $25v$, and $50v$) for each example, representing an upper bound on SelfIE performance.

We also procure **gold SAE labels** from Neuronpedia on the held-out SAE features. Note that the LM judge evaluates with respect to the same gold descriptions, meaning the gold SAE labels serve as a top-line number for the LM judge metric.

3.4 RESULTS

We report results for our trained explainers, as well as each of the baselines, in Table 1. Based on these results, we make several observations:

Trained explainers are effective. For every feature type and metric, training Llama-3.1-8B to explain itself outperforms all of the baselines by a significant margin. It even outperforms the gold

⁹The original SelfIE paper patches representations into the third layer, but prior work has found that patching into the first few layers work about equivalently well (which we also find). Thus, we patch every activation into the embedding layer.

¹⁰SelfIE prompts can be found in Section F.1.

SAE labels when scored via the simulator, due to noise in the ground-truth feature labels themselves (see error analysis in Section B.5).

For explainers, matching the subject matters more than parameter count. Among all trained models, the Llama-3.1-8B and Llama-3-8B models consistently performed the best across all four evaluations, while the Llama-3.1-8B-Instruct model was consistently a few (3-5) points behind. Meanwhile, the Qwen3-8B and the randomly-initialized Llama-3.1-70B model consistently performed the worst across all four evaluations, sometimes even underperforming baselines on the out-of-distribution evaluations. In this case, with Llama-3.1-8B as the target model, a Llama-3.1-8B explainer is significantly better than Llama-3.1-70B, showing that matching the target model matters more than a 9x increase in parameter count in this case.

Similar models are better explainers. More generally, we observe that models closest in architecture and training regimen to Llama-3.1-8B perform the best, while models that deviate in one or both perform worse: Llama-3.1-8B and Llama-3-8B share architecture and deviate slightly in pre-training, while Llama-3.1-8B-Instruct has the same architecture but has an additional instruction-tuning step. Qwen3-8B and Llama-3.1-70B both deviate completely in either training regimen or architecture, with Qwen3-8B differing significantly in training (but having a similar architecture) and Llama-3.1-70B differing in architecture (but sharing similar pre-training regimen).

Alignment between activations improves verbalization capability. To formalize the observation above, one way of quantifying the privileged access hypothesis is to posit that activation similarity between the explainer and target model predicts explainer performance. To investigate this, we compare the explanation capabilities of Llama-3.1-70b with both *pre-trained* projection and *randomly initialized* projection as a proxy for maximally and minimally aligned activation, respectively, given the model. As reported in Table 1, we can recover a significant fraction of performance when we start training from the pre-trained projection, performing 15% better on SAE explanations, 2.7 times better on real activations, and 1.7 times better on activation differences.

Additionally, we quantify the activation similarity of (a subset of) models reported in Table 1 with respect to the target model, and plot activation similarity vs. explainer performance. These plots can be found in Section B.2. Visually, they suggest that activation alignment is correlated with privileged access, in line with our findings above.

Taken together, these findings lead us to the following conclusion:

In feature description tasks, models’ privileged access to their internals improves explanations: they are better explained by fine-tuned versions of themselves than by other models.

Error Analysis. Finally, we performed a qualitative error analysis of 100 samples where the LM judge scored the explainer’s prediction as 0 (details in Section B.5). We found that most errors stem from issues in the “gold” SAE labels from Neuronpedia (consistent with our finding that Llama-3.1-8B can outperform the gold labels), LM judge scoring inconsistencies, and inherent prediction difficulty from sparsely activating features. Only 27% of errors are attributed to genuine explainer failures.

4 PRIVILEGED ACCESS CONFERS DATA-EFFICIENCY

To answer where and why privileged access may be useful, we investigate whether it confers data-efficiency advantages over alternatives. We train Llama-3.1-8B, Qwen3-8B, and the nearest neighbor baseline on subsets of the training data of various sizes and investigate scaling trends. The scaling curve for the held-out SAE features (LM judge evaluation) is reported in Figure 5, while the scaling curves for the other metrics and evaluation settings can be found in Figure 7.

Generally speaking, self-explanation is more data-efficient than either training another explainer model or nearest neighbors. At 0.8% of all training features (training on only 1024 samples per layer), Llama is already at 71% of its end-performance. Qwen is only at 35% of its end-performance and both forms of nearest neighbors (within- and across-layer) are at 55% of their end-performance. Note that the end-performance of Llama is already higher than both Qwen and nearest neighbors, meaning this gap is further amplified in the low data regime. Llama at 0.8% of training features

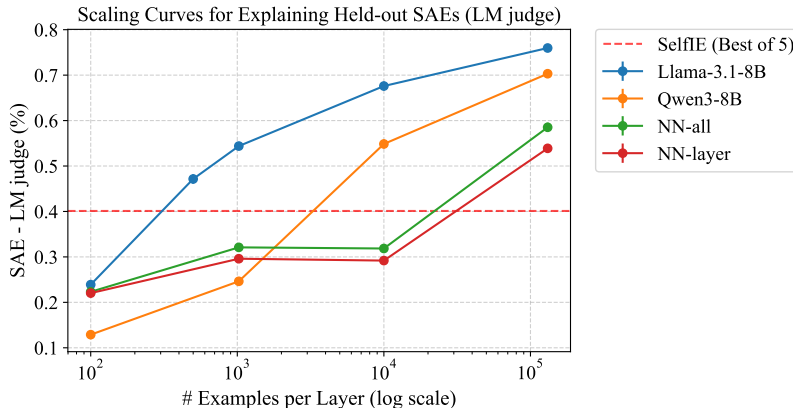


Figure 5: **Training self-as-explainer is more data-efficient than alternatives.** We plot scaling curves of each explainer: the number of training samples per layer is plotted against explanation quality, as judged by a LM judge on held-out SAE features. We find that matching the explainer to the target (Llama-3.1-8B) is generally the most data-efficient, while using another model as explainer (Qwen) or any form of nearest neighbor is much less effective in low-data regimes, taking over 1k-10k samples per layer to beat an untrained SelfIE baseline.

achieves 92.9% of the end-performance of all-layer nearest neighbors and 77.4% of fully-trained Qwen. These results indicate that:

Training a model to generate descriptions of its own features is data-efficient, particularly compared to training other models to describe the target model’s features.

This data-efficiency underscores the practical utility of self-explanation: annotating feature descriptions is expensive, and self-explanation training allows us to recover most of the performance with orders of magnitude less data. Figure 5 shows that retrieving the top-1 SAE feature (i.e. nearest neighbors) from a feature dictionary of 32k samples per layer performs comparably to a self-explainer model trained on only 1k samples per layer—over a hundred times fewer features.

Finally, we speculate that the small amount of required data reflects what is minimally necessary to learn *consistency* between activation patterns and verbalizations: perhaps minimal training is necessary if models are simply reusing existing circuits that generate activation patterns for verbalization.

5 GENERALIZATION ACROSS TASKS

To check whether self-explanation training and the privileged access hypothesis can be extended to other domains, we run preliminary experiments for two additional explanation types: predicting the outcomes of activation patching (§2.3) and input ablation (§2.4).

5.1 ACTIVATION PATCHING: TRAINING LMS TO PREDICT THE OUTCOMES OF ACTIVATION INTERVENTIONS

We examine models’ ability to explain results from activation patching experiments, which perturbs various parts of model components and examines which cause a change to the model output. This method is described in detail in Section 2.3. We train two different explainer models—Llama-3.1-8B and Qwen3-8B—to explain each other as the target models, creating four different combinations of evaluation settings.

Training Data. We use the CounterFact dataset (Meng et al., 2022) as a source of counterfactual input pairs x, x' , which consists of a corpus of factual subject–relation–object sentences like *Paris (subject) is the capital of (relation) France (object)*. We prompt the model with the subject and relation and ask the model to predict the object. We then identify a counterfactual sentence x' with the

Target	Explainer	Exact Match	Has-Changed F1	Content Match
Qwen3-8B	Qwen3-8B	64.0 \pm 0.4	80.2 \pm 0.3	71.0 \pm 0.4
	– activation	59.9 \pm 0.4	76.5 \pm 0.4	68.6 \pm 0.4
	– layer	65.0 \pm 0.4	80.0 \pm 0.3	72.7 \pm 0.4
	– token	63.9 \pm 0.4	79.4 \pm 0.3	71.7 \pm 0.4
	Llama-3.1-8B	54.1 \pm 0.4	73.9 \pm 0.4	65.4 \pm 0.4
Llama-3.1-8B	Qwen-3-8B (Untrained)	5.02 \pm 0.2	24.4 \pm 0.8	18.78 \pm 0.3
	Llama-3.1-8B	48.6 \pm 0.7	77.5 \pm 0.6	54.6 \pm 0.7
	– activation	45.2 \pm 0.7	73.9 \pm 0.6	50.8 \pm 0.7
	– layer	49.7 \pm 0.7	76.9 \pm 0.6	55.7 \pm 0.7
	– token	47.3 \pm 0.7	76.1 \pm 0.6	53.4 \pm 0.7
	Qwen3-8B	41.7 \pm 0.7	75.1 \pm 0.6	47.6 \pm 0.7
Llama-3.1-8B	Llama-3.1-8B (Untrained)	3.2 \pm 0.1	31.4 \pm 0.4	7.0 \pm 0.2

Table 2: **A target model’s activation patching outcomes are best predicted by itself.** We train Qwen3-8B and Llama-3.1-8B to verbalize their own activation patching outcomes, and compare against training the other model to explain their outcomes, and also against untrained versions of themselves. Scores (mean \pm standard error) are reported for three metrics—exact match, has-changed F1, and content prediction. For each target model and metric, **bold** indicates no significant difference from the best entry (paired t -test, $p \geq 0.05$). We also conduct experiments ablating the activation, layer, and token information from the explainer’s input. Ablating layer and token each have negligible effect, potentially because they can already be inferred from the activation.

same relation but differing subject and object (*Rome is the capital of*) and measure whether the most likely LM prediction changes (e.g. to *Italy*). We perform sampling to ensure an even split between changed and unchanged predictions, at each token position and layer chunk. See Section E.2 for details.

Baselines. To measure the effect of fine-tuning, we prompt the pre-trained Qwen3-8B and Llama-3.1-8B models (without any explanation training) to generate explanations of the form described in Section 2.3. The full prompts for zero-shot activation patching can be found in Section F.2. This is the analogous setting to the SelfIE baseline for feature description.

Metrics. Recall from Section 2.3 that the explainer output typically includes two parts: whether the target output would change under intervention (*changes / remains unchanged*), and the content of the change (*to France*). Based on this, we report three different types of metrics:

1. Has-Changed F1: Measures correctness of the first part of the explainer’s prediction, of whether the target’s output would change under intervention. We report the Macro F1 scores over the “changed” and “unchanged” classes.
2. Content Match: Measures correctness of the second part of the explainer’s prediction, of whether the explainer correctly predicts the *content* of target model’s prediction under intervention.
3. Exact Match: Exact match accuracy between generated explanation and ground-truth explanation. Requires the explainer to correctly predict both parts.

Results for activation patching can be found in Table 2. We see that the privileged access hypothesis is supported: Llama-3.1-8B is best at explaining Llama-3.1-8B, while Qwen3-8B is best at explaining Qwen3-8B. All trained explainers perform better than their untrained versions, which generally guess the has-changed value randomly.

Ablations. In addition to training each explainer model on each target model, we perform a set of ablations to isolate which component(s) of the input the explainer learned to condition on. The explainer input consists of three components: the activation v to insert (– activations), the layers $\ell_{1:i}$

Target	Explainer	Exact Match	Has-Changed F1	Content Match
Llama-Inst.	Llama-Inst.	18.2 \pm 1.0	58.2 \pm 1.3	24.9 \pm 1.2
Qwen3-8B	Llama-Inst.	14.6 \pm 0.9	52.4 \pm 1.2	22.9 \pm 1.1
Llama-Inst.	Llama-Inst. (Untrained)	21.0 \pm 1.1	45.5 \pm 1.3	36.7 \pm 1.3
Qwen3-8B	Qwen3-8B	62.7 \pm 1.3	73.4 \pm 1.1	70.5 \pm 1.2
Llama-Inst.	Qwen3-8B	33.1 \pm 1.3	59.4 \pm 1.3	48.3 \pm 1.3
Qwen3-8B	Qwen3-8B (Untrained)	30.2 \pm 1.2	53.2 \pm 0.5	39.9 \pm 1.3

Table 3: **An explainer model can best explain its own input ablation outcomes.** We train Qwen3-8B and Llama-3.1-8B to verbalize their own input ablation outcomes, and compare against training to verbalize each other’s outcomes. We also report untrained models explaining themselves. Note this table is sorted by explainer rather than target unlike previous tables. Scores (mean \pm standard error) are reported for three metrics—exact match, has-changed F1, and content prediction. For each explainer model and metric, we **bold** all entries not significantly different from the best entry (paired t -test, $p \geq 0.05$). We find evidence of a different version of privileged access: models are better at explaining themselves than other models.

(– layer), and the token t of the target model to patch into (– token). We train the explainer model with each aspect of the input ablated (conditioning only on the other two components) to generate the ground-truth explanations.¹¹ Our ablation studies suggest found that performance is generally robust to ablating the layer and token annotations in the input prompt. We believe this is because layer and token information is generally recoverable from the activation and input context alone. As evidence for this, we train Llama-3.1-8B to decode the layer and token from which an activation comes from, and get 98.7% accuracy (see Section C.1).

5.2 INPUT ABLATIONS: TRAINING LMS TO DESCRIBE THEIR DECISION RULES

Similar to the activation patching experiments, we train two models—Llama-3.1-8B-Instruct and Qwen3-8B—on their own behaviors and the behaviors of each other as the target models. Using the methods described in Section 2.4, we train models to explain how withholding or including parts of target models’ *input* would affect the output prediction.

Training Data. Following recent work used to study faithful chain-of-thought (Chen et al., 2025), we give \mathcal{M} inputs in the form of a multiple-choice question c with an injected hint \tilde{x} , i.e. $x = [c, \tilde{x}]$, and train the explainer to predict whether \mathcal{M} ’s most likely next token will change to \tilde{x} . Previously, Chen et al. (2025) found that models fail to verbalize \tilde{x} in their chain-of-thought, despite \tilde{x} being critical to its prediction ($\mathcal{M}([c, \tilde{x}]) \neq \mathcal{M}(c)$). Thus, we investigate whether models can be trained to detect *when and how* their prediction will change depending on \tilde{x} ’s presence.

We use MMLU (Hendrycks et al., 2021) as the source of multiple-choice reasoning question, and inject hints of the form $\tilde{x} = \text{“Hint: } A\text{”}$ to the end of the question. We randomly select \tilde{x} as one of the four multiple-choice options. To make the has-changed prediction nontrivial, we construct the hint prompt such that we have a roughly equal number of samples that change and do not change according to the hint. See Section E.3 for details.

Metrics. Recall from Section 2.4 that the explainer’s prediction involves two parts, similar to activation patching: whether the target’s prediction will change when the hint is removed (e.g. *output changes / output remains unchanged*), and the new prediction / content of the change (e.g. *to (A)*). Thus, we use the same three metrics as in activation patching (§5.1).

Baselines. Similar to Section 5.1, we include untrained explainer baselines. The prompt for then untrained models can be found in Section F.3.

¹¹Ablated prompts can be found in Section F.3.

Results are shown in Table 3. We find a different pattern of privileged access in this case, as Llama-3.1-8B appears to be an overall a much weaker explainer of both itself and of Qwen. However, when the *explainer* (instead of target) is held constant, both models are better at explaining themselves than explaining others: Llama is better at explaining Llama than Qwen (despite being a worse explainer overall), and vice versa. One way of viewing this is that privileged access is a significant first-order term in explainer performance, but can in some cases be overcome by other factors, such as a significant gap in the task-relevant capabilities of the explainer model.

One indication of Llama’s lack of capability comes from comparison to its untrained version: while Llama can learn to better predict its own has-changed value, its content match remains around random (25%) even after training.¹² If we only look at the has-changed F1, Llama’s ability to explain itself is on par with Qwen’s ability to explain it, despite Llama being a weaker overall explainer.

Finally, we examine untrained Qwen’s predictions and find that it a has-changed value of True only 0.4% of the time, and most of its content match comes from correctly predicting the unchanged answers (91.0% content match) compared to its changed answers (14.3% content match). This is consistent with findings on reasoning models in prior work: [Chen et al. \(2025\)](#) finds that no pre-trained LM would ever verbalize that it utilizes the hint, even when it did, similar to our finding that untrained Qwen never answers that its response changes based on the hint. This indicates that explicit fine-tuning is essential to elicit models to verbalize their true decision process.

Taken together, results on these two tasks show that:

Privileged access extends across tasks, but requires a certain model capacity; some models may be (model-agnostic) poor explainers of certain types of computation.

6 RELATED WORK

6.1 CHAIN-OF-THOUGHT FAITHFULNESS

Language models can be asked to verbalize their thought processes through chain-of-thought prompting, which offers a way for external monitoring ([Korbak et al., 2025](#); [Baker et al., 2025](#)), but prior work has found that these verbalizations can be unfaithful to their true decision-making processes ([Turpin et al., 2023](#); [Lanham et al., 2023](#); [Barez et al., 2025](#); [Chen et al., 2025](#)). This line of work directly inspires our hint ablation task setup, while our work attempts to remedy the unfaithfulness through a training objective that enforces consistency between model verbalization and their actual mechanisms.

6.2 MECHANISTIC INTERPRETABILITY METHODS

The field of mechanistic interpretability sets out to (1) describe individual features and (2) connect them to construct a causal circuit that performs a certain task. While many researchers have found success doing so manually in a fine-grained way both on the neuron level ([Gurnee et al., 2024](#)) and the circuit level for toy tasks ([Wang et al., 2023](#); [Nanda et al., 2023](#)), these methods have been challenging to scale and generalize to new models and tasks ([Sharkey et al., 2025](#)). To address scalability, automated feature description pipelines ([Hernandez et al., 2022](#); [Bills et al., 2023](#); [Choi et al., 2024](#); [Paulo et al., 2025](#)) and circuit discovery techniques ([Conmy et al., 2023](#); [Syed et al., 2024](#); [Hanna et al., 2024](#); [Hsu et al., 2025](#)) have been introduced that require substantial computational resources. Designing a scalable interpretability method that balances correctness/robustness and efficiency is an active area of research, one of which is attribution patching that use gradients to approximate important components to the output ([Nanda, 2023](#); [Syed et al., 2024](#)).

Closely related to the current study, one family of scalable interpretability methods attempts to leverage models’ own verbalization ability without any additional training. LogitLens ([nostalgebraist](#),

¹²Although untrained Llama’s content match is above random, a closer investigation reveals that it’s simply predicting the same content as the hint 81.9% of the time. This results in an above-random content match because if the model prediction remains unchanged, it typically is because the model’s original prediction matches the hint; we do not take the metric as evidence that untrained Llama is doing something non-trivial.

2020), PatchScopes (Ghandeharioun et al., 2024), SelfIE (Chen et al., 2024a) enable models to self-interpret zero-shot, but such methods require significant hyperparameter tuning (Kharlapenko et al., 2024). Pan et al. (2024) introduces Latent Interpretation Tuning, which fine-tunes models to answer questions about other models’ inputs via their hidden representations. We expand on this line of work by training models to self-verbalize their internals based on data collected from existing interpretability techniques that provide finer-grained pictures of models’ internal computations.

Finally, explanations based on special interpretability techniques are difficult for non-expert users to access, potentially requiring developers integrate many specialized interfaces (Viégas & Wattenberg, 2023; Chen et al., 2024b). Our work offers an alternative path toward user understanding, in which explanations can be provided “in-band” rather than via an external interface.

6.3 INTROSPECTION & METACOGNITION

Recent work investigates whether models possess *metacognition* or *introspective abilities* (Binder et al., 2025; Treutlein et al., 2024; Laine et al., 2024; Comsa & Shanahan, 2025; Plunkett et al., 2025). A central debate in this literature concerns whether models have privileged access to their internals, or whether introspection merely reflects their strong predictive capacity to learn external correlations (Song et al., 2025a;b; Li et al., 2025). We add to the literature by assessing models’ introspective abilities on their own *mechanisms* derived from mechanistic interpretability methods.

7 DISCUSSION: SELF-CONSISTENCY AS A FRAMEWORK FOR INTERPRETABILITY AND FAITHFULNESS

This paper explores improving model faithfulness and interpretability by training models to generate explanations consistent with outcomes of interpretability procedures. Across two question types, we find evidence that generated explanations take advantage of models’ privileged access to their own internal mechanisms, and on the third, we find evidence of explainer models having privileged *target* access to their own internals. Quantifying how factors such as explainer model capacity, target model complexity, task difficulty, etc. influence the emergence or manifestation of privileged access remains an important question for future work.

In a general sense, our results suggest that objectives that enforce *self-consistency* between models’ behavior and explanations may provide an avenue towards more scalable interpretability methods, faithful explanations, and alignment guarantees. The experiments in this paper derived (self-)explanation objectives from feature description, activation patching and input ablation techniques. Generalized versions of these objectives could in principle be applied to any method for generating ground-truth descriptions of model computation or behavior, e.g. to describe inferred user traits, surface adversarial triggers, or summarize influential training examples (Chen et al., 2024b; Wallace et al., 2019; Koh & Liang, 2017).

One natural extension would also optimize for consistency in a stronger sense: rather than having fine-tuned explainer models explain static target models, enforce that the target model is always identical to the explainer model. Perhaps more interestingly, these objectives could be applied in the *reverse* direction, fine-tuning models so that their behavior matches generated explanations, which might be normatively correct even if inaccurate as descriptions of models themselves. Applied in this way, consistency fine-tuning could provide a new mechanism for “unsupervised alignment” without relying on large preference datasets or reinforcement learning procedures.

ACKNOWLEDGMENTS

We would like to thank Dami Choi for technical support at early stages of this project. This work was supported by the Open Philanthropy Foundation and the MIT Quest for Intelligence. BZL is additionally funded by a Clare Boothe Luce Fellowship, and JA is funded by a Sloan Fellowship.

REFERENCES

Bowen Baker, Joost Huizinga, Leo Gao, Zehao Dou, Melody Y. Guan, Aleksander Madry, Wojciech Zaremba, Jakub Pachocki, and David Farhi. Monitoring reasoning models for misbehavior and

- the risks of promoting obfuscation, 2025. URL <https://arxiv.org/abs/2503.11926>.
- Fazl Barez, Tung-Yu Wu, Iván Arcuschin, Michael Lan, Vincent Wang, Noah Siegel, Nicolas Collignon, Clement Neo, Isabelle Lee, Alasdair Paren, Adel Bibi, Robert Trager, Damiano Fornasiere, John Yan, Yanai Elazar, and Yoshua Bengio. Chain-of-thought is not explainability, 2025. URL https://aigi.ox.ac.uk/wp-content/uploads/2025/07/Cot_Is_Not_Explainability.pdf. Preprint. Under review.
- David Bau, Jun-Yan Zhu, Hendrik Strobelt, Agata Lapedriza, Bolei Zhou, and Antonio Torralba. Understanding the role of individual units in a deep neural network. *Proceedings of the National Academy of Sciences*, 2020. ISSN 0027-8424. doi: 10.1073/pnas.1907375117. URL <https://www.pnas.org/content/early/2020/08/31/1907375117>.
- Steven Bills, Nick Cammarata, Dan Mossing, Henk Tillman, Leo Gao, Gabriel Goh, Ilya Sutskever, Jan Leike, Jeff Wu, and William Saunders. Language models can explain neurons in language models. <https://openaipublic.blob.core.windows.net/neuron-explainer/paper/index.html>, 2023.
- Felix Jedidja Binder, James Chua, Tomek Korbak, Henry Sleight, John Hughes, Robert Long, Ethan Perez, Miles Turpin, and Owain Evans. Looking inward: Language models can learn about themselves by introspection. In *The Thirteenth International Conference on Learning Representations*, 2025. URL <https://openreview.net/forum?id=eb5pkwIB5i>.
- Trenton Bricken, Adly Templeton, Joshua Batson, Brian Chen, Adam Jermyn, Tom Conerly, Nick Turner, Cem Anil, Carson Denison, Amanda Askell, Robert Lasenby, Yifan Wu, Shauna Kravec, Nicholas Schiefer, Tim Maxwell, Nicholas Joseph, Zac Hatfield-Dodds, Alex Tamkin, Karina Nguyen, Brayden McLean, Josiah E Burke, Tristan Hume, Shan Carter, Tom Henighan, and Christopher Olah. Towards monosemanticity: Decomposing language models with dictionary learning. *Transformer Circuits Thread*, 2023. <https://transformer-circuits.pub/2023/monosemantic-features/index.html>.
- Yurui Chang, Bochuan Cao, Yujia Wang, Jinghui Chen, and Lu Lin. JoPA: Explaining large language model’s generation via joint prompt attribution. In Wanxiang Che, Joyce Nabende, Ekaterina Shutova, and Mohammad Taher Pilehvar (eds.), *Proceedings of the 63rd Annual Meeting of the Association for Computational Linguistics (Volume 1: Long Papers)*, pp. 22106–22122, Vienna, Austria, July 2025. Association for Computational Linguistics. ISBN 979-8-89176-251-0. doi: 10.18653/v1/2025.acl-long.1074. URL <https://aclanthology.org/2025.acl-long.1074/>.
- Haozhe Chen, Carl Vondrick, and Chengzhi Mao. SelfIE: Self-interpretation of large language model embeddings. In *Forty-first International Conference on Machine Learning*, 2024a. URL <https://openreview.net/forum?id=gjgRkYR7>.
- Yanda Chen, Joe Benton, Ansh Radhakrishnan, Jonathan Uesato, Carson Denison, John Schulman, Arushi Somani, Peter Hase, Misha Wagner, Fabien Roger, Vlad Mikulik, Samuel R. Bowman, Jan Leike, Jared Kaplan, and Ethan Perez. Reasoning models don’t always say what they think, 2025. URL <https://arxiv.org/abs/2505.05410>.
- Yida Chen, Aoyu Wu, Trevor DePodesta, Catherine Yeh, Kenneth Li, Nicholas Castillo Marin, Oam Patel, Jan Riecke, Shivam Raval, Olivia Seow, Martin Wattenberg, and Fernanda Viégas. Designing a dashboard for transparency and control of conversational AI, 2024b. URL <https://arxiv.org/abs/2406.07882>.
- Dami Choi, Vincent Huang, Kevin Meng, Daniel D Johnson, Jacob Steinhardt, and Sarah Schwettmann. Scaling automatic neuron description. <https://transluce.org/neuron-descriptions>, October 2024.
- Iulia M. Comsa and Murray Shanahan. Does it make sense to speak of introspection in large language models?, 2025. URL <https://arxiv.org/abs/2506.05068>.
- Arthur Conmy, Augustine N. Mavor-Parker, Aengus Lynch, Stefan Heimersheim, and Adrià Garriga-Alonso. Towards automated circuit discovery for mechanistic interpretability. In *Thirty-seventh Conference on Neural Information Processing Systems*, 2023.

- Ian C. Covert, Scott Lundberg, and Su-In Lee. Understanding global feature contributions with additive importance measures. In *Proceedings of the 34th International Conference on Neural Information Processing Systems, NIPS '20*, Red Hook, NY, USA, 2020. Curran Associates Inc. ISBN 9781713829546.
- Nelson Elhage, Tristan Hume, Catherine Olsson, Nicholas Schiefer, Tom Henighan, Shauna Kravec, Zac Hatfield-Dodds, Robert Lasenby, Dawn Drain, Carol Chen, Roger Grosse, Sam McCandlish, Jared Kaplan, Dario Amodei, Martin Wattenberg, and Christopher Olah. Toy models of superposition. *Transformer Circuits Thread*, 2022. https://transformer-circuits.pub/2022/toy_model/index.html.
- Gemma Team, Morgane Riviere, Shreya Pathak, Pier Giuseppe Sessa, Cassidy Hardin, Surya Bhupatiraju, Léonard Hussenot, Thomas Mesnard, Bobak Shahriari, Alexandre Ramé, Johan Ferret, Peter Liu, Pouya Tafti, Abe Friesen, Michelle Casbon, Sabela Ramos, Ravin Kumar, Charline Le Lan, Sammy Jerome, Anton Tsitsulin, Nino Vieillard, Piotr Stanczyk, Sertan Girgin, Nikola Momchev, Matt Hoffman, Shantanu Thakoor, Jean-Bastien Grill, Behnam Neyshabur, Olivier Bachem, Alanna Walton, Aliaksei Severyn, Alicia Parrish, Aliya Ahmad, Allen Hutchison, Alvin Abdagic, Amanda Carl, Amy Shen, Andy Brock, Andy Coenen, Anthony Laforge, Antonia Paterson, Ben Bastian, Bilal Piot, Bo Wu, Brandon Royal, Charlie Chen, Chintu Kumar, Chris Perry, Chris Welty, Christopher A. Choquette-Choo, Danila Sinopalnikov, David Weinberger, Dimple Vijaykumar, Dominika Rogozińska, Dustin Herbison, Elisa Bandy, Emma Wang, Eric Noland, Erica Moreira, Evan Senter, Evgenii Eltyshev, Francesco Visin, Gabriel Rasskin, Gary Wei, Glenn Cameron, Gus Martins, Hadi Hashemi, Hanna Klimczak-Plucińska, Harleen Batra, Harsh Dhand, Ivan Nardini, Jacinda Mein, Jack Zhou, James Svensson, Jeff Stanway, Jetha Chan, Jin Peng Zhou, Joana Carrasqueira, Joana Iljazi, Jocelyn Becker, Joe Fernandez, Joost van Amersfoort, Josh Gordon, Josh Lipschultz, Josh Newlan, Ju yeong Ji, Kareem Mohamed, Kartikeya Badola, Kat Black, Katie Millican, Keelin McDonnell, Kelvin Nguyen, Kiranbir Sodhia, Kish Greene, Lars Lowe Sjoesund, Lauren Usui, Laurent Sifre, Lena Heuermann, Leticia Lago, Lilly McNealus, Livio Baldini Soares, Logan Kilpatrick, Lucas Dixon, Luciano Martins, Machel Reid, Manvinder Singh, Mark Iverson, Martin Görner, Mat Velloso, Mateo Wirth, Matt Davidow, Matt Miller, Matthew Rahtz, Matthew Watson, Meg Risdal, Mehran Kazemi, Michael Moynihan, Ming Zhang, Minsuk Kahng, Minwoo Park, Mofi Rahman, Mohit Khatwani, Natalie Dao, Nenshad Bardoliwalla, Nesh Devanathan, Neta Dumai, Nilay Chauhan, Oscar Wahltinez, Pankil Botarda, Parker Barnes, Paul Barham, Paul Michel, Pengchong Jin, Petko Georgiev, Phil Culliton, Pradeep Kuppala, Ramona Comanescu, Ramona Merhej, Reena Jana, Reza Ardeshtir Rokni, Rishabh Agarwal, Ryan Mullins, Samaneh Saadat, Sara Mc Carthy, Sarah Cogan, Sarah Perrin, Sébastien M. R. Arnold, Sebastian Krause, Shengyang Dai, Shruti Garg, Shruti Sheth, Sue Rostrom, Susan Chan, Timothy Jordan, Ting Yu, Tom Eccles, Tom Hennigan, Tomas Kocisky, Tulsee Doshi, Vihan Jain, Vikas Yadav, Vilobh Meshram, Vishal Dharmadhikari, Warren Barkley, Wei Wei, Wenming Ye, Woohyun Han, Woosuk Kwon, Xiang Xu, Zhe Shen, Zhitao Gong, Zichuan Wei, Victor Cotruta, Phoebe Kirk, Anand Rao, Minh Giang, Ludovic Peran, Tris Warkentin, Eli Collins, Joelle Barral, Zoubin Ghahramani, Raia Hadsell, D. Sculley, Jeanine Banks, Anca Dragan, Slav Petrov, Oriol Vinyals, Jeff Dean, Demis Hassabis, Koray Kavukcuoglu, Clement Faret, Elena Buchatskaya, Sebastian Borgeaud, Noah Fiedel, Armand Joulin, Kathleen Kenealy, Robert Dadashi, and Alek Andreev. Gemma 2: Improving open language models at a practical size, 2024. URL <https://arxiv.org/abs/2408.00118>.
- Asma Ghandeharioun, Avi Caciularu, Adam Pearce, Lucas Dixon, and Mor Geva. Patchscopes: A unifying framework for inspecting hidden representations of language models. In *Forty-first International Conference on Machine Learning*, 2024. URL <https://openreview.net/forum?id=5uwBzcn885>.
- Aaron Grattafiori, Abhimanyu Dubey, Abhinav Jauhri, Abhinav Pandey, Abhishek Kadian, Ahmad Al-Dahle, Aiesha Letman, Akhil Mathur, Alan Schelten, Alex Vaughan, Amy Yang, Angela Fan, Anirudh Goyal, Anthony Hartshorn, Aobo Yang, Archi Mitra, Archie Sravankumar, Artem Korotnev, Arthur Hinsvark, Arun Rao, Aston Zhang, Aurelien Rodriguez, Austen Gregerson, Ava Spataru, Baptiste Roziere, Bethany Biron, Binh Tang, Bobbie Chern, Charlotte Caucheteux, Chaya Nayak, Chloe Bi, Chris Marra, Chris McConnell, Christian Keller, Christophe Touret, Chunyang Wu, Corinne Wong, Cristian Canton Ferrer, Cyrus Nikolaidis, Damien Allonsius, Daniel Song, Danielle Pintz, Danny Livshits, Danny Wyatt, David Esiobu, Dhruv Choudhary,

Dhruv Mahajan, Diego Garcia-Olano, Diego Perino, Dieuwke Hupkes, Egor Lakomkin, Ehab AlBadawy, Elina Lobanova, Emily Dinan, Eric Michael Smith, Filip Radenovic, Francisco Guzmán, Frank Zhang, Gabriel Synnaeve, Gabrielle Lee, Georgia Lewis Anderson, Govind Thattai, Graeme Nail, Gregoire Mialon, Guan Pang, Guillem Cucurell, Hailey Nguyen, Hannah Korevaar, Hu Xu, Hugo Touvron, Iliyan Zarov, Imanol Arrieta Ibarra, Isabel Kloumann, Ishan Misra, Ivan Evtimov, Jack Zhang, Jade Copet, Jaewon Lee, Jan Geffert, Jana Vranes, Jason Park, Jay Mahadeokar, Jeet Shah, Jelmer van der Linde, Jennifer Billock, Jenny Hong, Jenya Lee, Jeremy Fu, Jianfeng Chi, Jianyu Huang, Jiawen Liu, Jie Wang, Jiecao Yu, Joanna Bitton, Joe Spisak, Jongsoo Park, Joseph Rocca, Joshua Johnstun, Joshua Saxe, Junteng Jia, Kalyan Vasuden Alwala, Karthik Prasad, Kartikeya Upasani, Kate Plawiak, Ke Li, Kenneth Heafield, Kevin Stone, Khalid El-Arini, Krithika Iyer, Kshitiz Malik, Kuenley Chiu, Kunal Bhalla, Kushal Lakhota, Lauren Rantala-Yearly, Laurens van der Maaten, Lawrence Chen, Liang Tan, Liz Jenkins, Louis Martin, Lovish Madaan, Lubo Malo, Lukas Blecher, Lukas Landzaat, Luke de Oliveira, Madeline Muzzi, Mahesh Paspuleti, Mannat Singh, Manohar Paluri, Marcin Kardas, Maria Tsimpoukelli, Mathew Oldham, Mathieu Rita, Maya Pavlova, Melanie Kambadur, Mike Lewis, Min Si, Mitesh Kumar Singh, Mona Hassan, Naman Goyal, Narjes Torabi, Nikolay Bashlykov, Nikolay Bogoychev, Niladri Chatterji, Ning Zhang, Olivier Duchenne, Onur Çelebi, Patrick Alrassy, Pengchuan Zhang, Pengwei Li, Petar Vasic, Peter Weng, Prajjwal Bhargava, Pratik Dubal, Praveen Krishnan, Punit Singh Koura, Puxin Xu, Qing He, Qingxiao Dong, Ragavan Srinivasan, Raj Ganapathy, Ramon Calderer, Ricardo Silveira Cabral, Robert Stojnic, Roberta Raileanu, Rohan Maheswari, Rohit Girdhar, Rohit Patel, Romain Sauvestre, Ronnie Polidoro, Roshan Sumbaly, Ross Taylor, Ruan Silva, Rui Hou, Rui Wang, Saghar Hosseini, Sahana Chennabasappa, Sanjay Singh, Sean Bell, Seohyun Sonia Kim, Sergey Edunov, Shaoliang Nie, Sharan Narang, Sharath Rapparthi, Sheng Shen, Shengye Wan, Shruti Bhosale, Shun Zhang, Simon Vandenhende, Soumya Batra, Spencer Whitman, Sten Sootla, Stephane Collet, Suchin Gururangan, Sydney Borodinsky, Tamar Herman, Tara Fowler, Tarek Sheasha, Thomas Georgiou, Thomas Scialom, Tobias Speckbacher, Todor Mihaylov, Tong Xiao, Ujjwal Karn, Vedanuj Goswami, Vibhor Gupta, Vignesh Ramanathan, Viktor Kerkez, Vincent Gonguet, Virginie Do, Vish Vogeti, Vitor Albiero, Vladan Petrovic, Weiwei Chu, Wenhan Xiong, Wenyin Fu, Whitney Meers, Xavier Martinet, Xiaodong Wang, Xiaofang Wang, Xiaoqing Ellen Tan, Xide Xia, Xinfeng Xie, Xuchao Jia, Xuewei Wang, Yaelle Goldschlag, Yashesh Gaur, Yasmine Babaei, Yi Wen, Yiwen Song, Yuchen Zhang, Yue Li, Yuning Mao, Zacharie Delpierre Coudert, Zheng Yan, Zhengxing Chen, Zoe Papanikos, Aaditya Singh, Aayushi Srivastava, Abha Jain, Adam Kelsey, Adam Shajnfeld, Adithya Gangidi, Adolfo Victoria, Ahuva Goldstand, Ajay Menon, Ajay Sharma, Alex Boesenberg, Alexei Baevski, Allie Feinstein, Amanda Kallet, Amit Sangani, Amos Teo, Anam Yunus, Andrei Lupu, Andres Alvarado, Andrew Caples, Andrew Gu, Andrew Ho, Andrew Poulton, Andrew Ryan, Ankit Ramchandani, Annie Dong, Annie Franco, Anuj Goyal, Aparajita Saraf, Arkabandhu Chowdhury, Ashley Gabriel, Ashwin Bharambe, Assaf Eisenman, Azadeh Yazdan, Beau James, Ben Maurer, Benjamin Leonhardi, Bernie Huang, Beth Loyd, Beto De Paola, Bhargavi Paranjape, Bing Liu, Bo Wu, Boyu Ni, Braden Hancock, Bram Wasti, Brandon Spence, Brani Stojkovic, Brian Gamido, Britt Montalvo, Carl Parker, Carly Burton, Catalina Mejia, Ce Liu, Changhan Wang, Changkyu Kim, Chao Zhou, Chester Hu, Ching-Hsiang Chu, Chris Cai, Chris Tindal, Christoph Feichtenhofer, Cynthia Gao, Damon Civin, Dana Beaty, Daniel Kreymer, Daniel Li, David Adkins, David Xu, Davide Testuggine, Delia David, Devi Parikh, Diana Liskovich, Didem Foss, Dingkan Wang, Duc Le, Dustin Holland, Edward Dowling, Eissa Jamil, Elaine Montgomery, Eleonora Presani, Emily Hahn, Emily Wood, Eric-Tuan Le, Erik Brinkman, Esteban Arcaute, Evan Dunbar, Evan Smothers, Fei Sun, Felix Kreuk, Feng Tian, Filippos Kokkinos, Firat Ozgenel, Francesco Caggioni, Frank Kanayet, Frank Seide, Gabriela Medina Florez, Gabriella Schwarz, Gada Badeer, Georgia Swee, Gil Halpern, Grant Herman, Grigory Sizov, Guangyi, Zhang, Guna Lakshminarayanan, Hakan Inan, Hamid Shojanazeri, Han Zou, Hannah Wang, Hanwen Zha, Haroun Habeeb, Harrison Rudolph, Helen Suk, Henry Aspegren, Hunter Goldman, Hongyuan Zhan, Ibrahim Damlaj, Igor Molybog, Igor Tufanov, Ilias Leontiadis, Irina-Elena Veliche, Itai Gat, Jake Weissman, James Geboski, James Kohli, Janice Lam, Japhet Asher, Jean-Baptiste Gaya, Jeff Marcus, Jeff Tang, Jennifer Chan, Jenny Zhen, Jeremy Reizenstein, Jeremy Teboul, Jessica Zhong, Jian Jin, Jingyi Yang, Joe Cummings, Jon Carvill, Jon Sheppard, Jonathan McPhie, Jonathan Torres, Josh Ginsburg, Junjie Wang, Kai Wu, Kam Hou U, Karan Saxena, Kartikay Khandelwal, Katayoun Zand, Kathy Matosich, Kaushik Veeraraghavan, Kelly Michelena, Keqian Li, Kiran Jagadeesh, Kun Huang, Kunal Chawla, Kyle Huang, Lailin Chen, Lakshya Garg, Lavender A, Leandro Silva, Lee Bell, Lei Zhang, Liangpeng Guo, Licheng Yu, Liron Moshkovich, Luca Wehrstedt, Madian Khabsa,

- Manav Avalani, Manish Bhatt, Martynas Mankus, Matan Hasson, Matthew Lennie, Matthias Reso, Maxim Groshev, Maxim Naumov, Maya Lathi, Meghan Keneally, Miao Liu, Michael L. Seltzer, Michal Valko, Michelle Restrepo, Mihir Patel, Mik Vyatskov, Mikayel Samvelyan, Mike Clark, Mike Macey, Mike Wang, Miquel Jubert Hermoso, Mo Metanat, Mohammad Rastegari, Munish Bansal, Nandhini Santhanam, Natascha Parks, Natasha White, Navyata Bawa, Nayan Singhal, Nick Egebo, Nicolas Usunier, Nikhil Mehta, Nikolay Pavlovich Laptev, Ning Dong, Norman Cheng, Oleg Chernoguz, Olivia Hart, Omkar Salpekar, Ozlem Kalinli, Parkin Kent, Parth Parekh, Paul Saab, Pavan Balaji, Pedro Rittner, Philip Bontrager, Pierre Roux, Piotr Dollar, Polina Zvyagina, Prashant Ratanchandani, Pritish Yuvraj, Qian Liang, Rachad Alao, Rachel Rodriguez, Rafi Ayub, Raghotham Murthy, Raghu Nayani, Rahul Mitra, Rangaprabhu Parthasarathy, Raymond Li, Rebekkah Hogan, Robin Battey, Rocky Wang, Russ Howes, Ruty Rinott, Sachin Mehta, Sachin Siby, Sai Jayesh Bondu, Samyak Datta, Sara Chugh, Sara Hunt, Sargun Dhillon, Sasha Sidorov, Satadru Pan, Saurabh Mahajan, Saurabh Verma, Seiji Yamamoto, Sharadh Ramaswamy, Shaun Lindsay, Sheng Feng, Shenghao Lin, Shengxin Cindy Zha, Shishir Patil, Shiva Shankar, Shuqiang Zhang, Sinong Wang, Sneha Agarwal, Soji Sajuyigbe, Soumith Chintala, Stephanie Max, Stephen Chen, Steve Kehoe, Steve Satterfield, Sudarshan Govindaprasad, Sumit Gupta, Summer Deng, Sungmin Cho, Sunny Virk, Suraj Subramanian, Sy Choudhury, Sydney Goldman, Tal Remez, Tamar Glaser, Tamara Best, Thilo Koehler, Thomas Robinson, Tianhe Li, Tianjun Zhang, Tim Matthews, Timothy Chou, Tzook Shaked, Varun Vontimitta, Victoria Ajayi, Victoria Montanez, Vijai Mohan, Vinay Satish Kumar, Vishal Mangla, Vlad Ionescu, Vlad Poenaru, Vlad Tiberiu Mihailescu, Vladimir Ivanov, Wei Li, Wenchen Wang, Wenwen Jiang, Wes Bouaziz, Will Constable, Xiaocheng Tang, Xiaojian Wu, Xiaolan Wang, Xilun Wu, Xinbo Gao, Yaniv Kleinman, Yanjun Chen, Ye Hu, Ye Jia, Ye Qi, Yenda Li, Yilin Zhang, Ying Zhang, Yossi Adi, Youngjin Nam, Yu, Wang, Yu Zhao, Yuchen Hao, Yundi Qian, Yunlu Li, Yuzi He, Zach Rait, Zachary DeVito, Zef Rosnbrick, Zhaoduo Wen, Zhenyu Yang, Zhiwei Zhao, and Zhiyu Ma. The Llama 3 herd of models, 2024. URL <https://arxiv.org/abs/2407.21783>.
- Wes Gurnee, Theo Horsley, Zifan Carl Guo, Tara Rezaei Kheirkhah, Qinyi Sun, Will Hathaway, Neel Nanda, and Dimitris Bertsimas. Universal neurons in GPT2 language models. *Transactions on Machine Learning Research*, 2024. ISSN 2835-8856. URL <https://openreview.net/forum?id=ZeI104QZ8I>.
- Michael Hanna, Sandro Pezzelle, and Yonatan Belinkov. Have faith in faithfulness: Going beyond circuit overlap when finding model mechanisms. In *ICML 2024 Workshop on Mechanistic Interpretability*, 2024. URL <https://openreview.net/forum?id=grXgesr5dT>.
- Zhengfu He, Wentao Shu, Xuyang Ge, Lingjie Chen, Junxuan Wang, Yunhua Zhou, Frances Liu, Qipeng Guo, Xuanjing Huang, Zuxuan Wu, Yu-Gang Jiang, and Xipeng Qiu. Llama scope: Extracting millions of features from Llama-3.1-8B with sparse autoencoders. *CoRR*, abs/2410.20526, 2024. URL <https://doi.org/10.48550/arXiv.2410.20526>.
- Dan Hendrycks, Collin Burns, Steven Basart, Andy Zou, Mantas Mazeika, Dawn Song, and Jacob Steinhardt. Measuring massive multitask language understanding. *Proceedings of the International Conference on Learning Representations (ICLR)*, 2021.
- Evan Hernandez, Sarah Schwettmann, David Bau, Teona Bagashvili, Antonio Torralba, and Jacob Andreas. Natural language descriptions of deep visual features. In *International Conference on Learning Representations*, 2022. URL <https://arxiv.org/abs/2201.11114>.
- Aliyah R. Hsu, Georgia Zhou, Yeshwanth Cherapanamjeri, Yaxuan Huang, Anobel Odisho, Peter R. Carroll, and Bin Yu. Efficient automated circuit discovery in transformers using contextual decomposition. In *The Thirteenth International Conference on Learning Representations*, 2025. URL <https://openreview.net/forum?id=41H1N8XYM5>.
- Edward J Hu, yelong shen, Phillip Wallis, Zeyuan Allen-Zhu, Yuanzhi Li, Shean Wang, Lu Wang, and Weizhu Chen. LoRA: Low-rank adaptation of large language models. In *International Conference on Learning Representations*, 2022. URL <https://openreview.net/forum?id=nZeVKeeFYf9>.
- Robert Huben, Hoagy Cunningham, Logan Riggs Smith, Aidan Ewart, and Lee Sharkey. Sparse autoencoders find highly interpretable features in language models. In *The Twelfth International*

- Conference on Learning Representations*, 2024. URL <https://openreview.net/forum?id=F76bwRSLek>.
- Dmitrii Kharlapenko, Stepan Shabalín, Neel Nanda, and Arthur Conmy. Self-explaining SAE features. AI Alignment Forum, August 2024. URL <https://www.lesswrong.com/posts/>.
- Pang Wei Koh and Percy Liang. Understanding black-box predictions via influence functions. In Doina Precup and Yee Whye Teh (eds.), *Proceedings of the 34th International Conference on Machine Learning*, volume 70 of *Proceedings of Machine Learning Research*, pp. 1885–1894. PMLR, 06–11 Aug 2017. URL <https://proceedings.mlr.press/v70/koh17a.html>.
- Tomek Korbak, Mikita Balesni, Elizabeth Barnes, Yoshua Bengio, Joe Benton, Joseph Bloom, Mark Chen, Alan Cooney, Allan Dafoe, Anca Dragan, Scott Emmons, Owain Evans, David Farhi, Ryan Greenblatt, Dan Hendrycks, Marius Hobbhahn, Evan Hubinger, Geoffrey Irving, Erik Jenner, Daniel Kokotajlo, Victoria Krakovna, Shane Legg, David Lindner, David Luan, Aleksander Mądry, Julian Michael, Neel Nanda, Dave Orr, Jakub Pachocki, Ethan Perez, Mary Phuong, Fabien Roger, Joshua Saxe, Buck Shlegeris, Martín Soto, Eric Steinberger, Jasmine Wang, Wojciech Zaremba, Bowen Baker, Rohin Shah, and Vlad Mikulik. Chain of thought monitorability: A new and fragile opportunity for AI safety, 2025. URL <https://arxiv.org/abs/2507.11473>.
- Rudolf Laine, Bilal Chughtai, Jan Betley, Kaivalya Hariharan, Jeremy Scheurer, Mikita Balesni, Marius Hobbhahn, Alexander Meinke, and Owain Evans. Me, myself, and ai: The situational awareness dataset (sad) for llms, 2024. URL <https://arxiv.org/abs/2407.04694>.
- Tamera Lanham, Anna Chen, Ansh Radhakrishnan, Benoit Steiner, Carson Denison, Danny Hernandez, Dustin Li, Esin Durmus, Evan Hubinger, Jackson Kernion, Kamilė Lukošiuūtė, Karina Nguyen, Newton Cheng, Nicholas Joseph, Nicholas Schiefer, Oliver Rausch, Robin Larson, Sam McCandlish, Sandipan Kundu, Saurav Kadavath, Shannon Yang, Thomas Henighan, Timothy Maxwell, Timothy Telleen-Lawton, Tristan Hume, Zac Hatfield-Dodds, Jared Kaplan, Jan Brauner, Samuel R. Bowman, and Ethan Perez. Measuring faithfulness in chain-of-thought reasoning, 2023. URL <https://arxiv.org/abs/2307.13702>.
- Millicent Li, Alberto Mario Ceballos Arroyo, Giordano Rogers, Naomi Saphra, and Byron C Wallace. Do natural language descriptions of model activations convey privileged information? In *Mechanistic Interpretability Workshop at NeurIPS 2025*, 2025. URL <https://openreview.net/forum?id=zyhibAkzSA>.
- Tom Lieberum, Senthooran Rajamanoharan, Arthur Conmy, Lewis Smith, Nicolas Sonnerat, Vikrant Varma, Janos Kramar, Anca Dragan, Rohin Shah, and Neel Nanda. Gemma scope: Open sparse autoencoders everywhere all at once on Gemma 2. In Yonatan Belinkov, Najoung Kim, Jaap Jumelet, Hosein Mohebbi, Aaron Mueller, and Hanjie Chen (eds.), *Proceedings of the 7th Black-boxNLP Workshop: Analyzing and Interpreting Neural Networks for NLP*, pp. 278–300, Miami, Florida, US, November 2024. Association for Computational Linguistics. doi: 10.18653/v1/2024.blackboxnlp-1.19. URL <https://aclanthology.org/2024.blackboxnlp-1.19/>.
- Johnny Lin. Neuronpedia: Interactive reference and tooling for analyzing neural networks, 2023. URL <https://www.neuronpedia.org>. Software available from neuronpedia.org.
- Kevin Meng, David Bau, Alex Andonian, and Yonatan Belinkov. Locating and editing factual associations in GPT. *Advances in Neural Information Processing Systems*, 36, 2022. arXiv:2202.05262.
- Neel Nanda. Attribution patching: Activation patching at industrial scale. <https://www.neelnanda.io/mechanistic-interpretability/attribution-patching>, 2023. Accessed: 2025-10-30.
- Neel Nanda, Lawrence Chan, Tom Lieberum, Jess Smith, and Jacob Steinhardt. Progress measures for grokking via mechanistic interpretability, 2023. URL <https://arxiv.org/abs/2301.05217>.
- nostalgebraist. Interpreting GPT: the logit lens. LessWrong, August 2020. URL <https://www.lesswrong.com/posts/AcKRB8wDpdaN6v6ru/interpreting-gpt-the-logit-lens>.

- Alexander Pan, Lijie Chen, and Jacob Steinhardt. LatentQA: Teaching LLMs to decode activations into natural language. *arXiv*, 2024.
- Gonçalo Santos Paulo, Alex Troy Mallen, Caden Juang, and Nora Belrose. Automatically interpreting millions of features in large language models, 2025. URL <https://openreview.net/forum?id=51IXRf8Lnw>.
- Guilherme Penedo, Hynek Kydlíček, Loubna Ben allal, Anton Lozhkov, Margaret Mitchell, Colin Raffel, Leandro Von Werra, and Thomas Wolf. The FineWeb datasets: Decanting the web for the finest text data at scale. In *The Thirty-eight Conference on Neural Information Processing Systems Datasets and Benchmarks Track*, 2024. URL <https://openreview.net/forum?id=n6SCKn2QaG>.
- Dillon Plunkett, Adam Morris, Keerthi Reddy, and Jorge Morales. Self-interpretability: LLMs can describe complex internal processes that drive their decisions, 2025. URL <https://arxiv.org/abs/2505.17120>.
- Lee Sharkey, Bilal Chughtai, Joshua Batson, Jack Lindsey, Jeffrey Wu, Lucius Bushnaq, Nicholas Goldowsky-Dill, Stefan Heimersheim, Alejandro Ortega, Joseph Isaac Bloom, Stella Biderman, Adrià Garriga-Alonso, Arthur Conmy, Neel Nanda, Jessica Mary Rumbelow, Martin Wattenberg, Nandi Schoots, Joseph Miller, William Saunders, Eric J Michaud, Stephen Casper, Max Tegmark, David Bau, Eric Todd, Atticus Geiger, Mor Geva, Jesse Hoogland, Daniel Murfet, and Thomas McGrath. Open problems in mechanistic interpretability. *Transactions on Machine Learning Research*, 2025. ISSN 2835-8856. URL <https://openreview.net/forum?id=91H76m9Z94>. Survey Certification.
- Karen Simonyan, Andrea Vedaldi, and Andrew Zisserman. Deep inside convolutional networks: Visualising image classification models and saliency maps. *CoRR*, abs/1312.6034, 2013. URL <https://api.semanticscholar.org/CorpusID:1450294>.
- Siyuan Song, Jennifer Hu, and Kyle Mahowald. Language models fail to introspect about their knowledge of language. In *Second Conference on Language Modeling*, 2025a. URL <https://openreview.net/forum?id=AivRDOFi5H>.
- Siyuan Song, Harvey Lederman, Jennifer Hu, and Kyle Mahowald. Privileged self-access matters for introspection in AI, 2025b. URL <https://arxiv.org/abs/2508.14802>.
- Aaquib Syed, Can Rager, and Arthur Conmy. Attribution patching outperforms automated circuit discovery. In Yonatan Belinkov, Najoung Kim, Jaap Jumelet, Hosein Mohebbi, Aaron Mueller, and Hanjie Chen (eds.), *Proceedings of the 7th BlackboxNLP Workshop: Analyzing and Interpreting Neural Networks for NLP*, pp. 407–416, Miami, Florida, US, November 2024. Association for Computational Linguistics. doi: 10.18653/v1/2024.blackboxnlp-1.25. URL <https://aclanthology.org/2024.blackboxnlp-1.25/>.
- Adly Templeton, Tom Conerly, Jonathan Marcus, Jack Lindsey, Trenton Bricken, Brian Chen, Adam Pearce, Craig Citro, Emmanuel Ameisen, Andy Jones, Hoagy Cunningham, Nicholas L Turner, Callum McDougall, Monte MacDiarmid, C. Daniel Freeman, Theodore R. Sumers, Edward Rees, Joshua Batson, Adam Jermyn, Shan Carter, Chris Olah, and Tom Henighan. Scaling monosemanticity: Extracting interpretable features from Claude 3 Sonnet. *Transformer Circuits Thread*, 2024. URL <https://transformer-circuits.pub/2024/scaling-monosemanticity/index.html>.
- Johannes Treutlein, Dami Choi, Jan Betley, Samuel Marks, Cem Anil, Roger Baker Grosse, and Owain Evans. Connecting the dots: LLMs can infer and verbalize latent structure from disparate training data. In *The Thirty-eighth Annual Conference on Neural Information Processing Systems*, 2024. URL <https://openreview.net/forum?id=7FokMz6U8n>.
- Miles Turpin, Julian Michael, Ethan Perez, and Samuel R. Bowman. Language models don’t always say what they think: Unfaithful explanations in chain-of-thought prompting. In *Thirty-seventh Conference on Neural Information Processing Systems*, 2023. URL <https://openreview.net/forum?id=bzs4uPLXvi>.

- Keyon Vafa, Yuntian Deng, David Blei, and Alexander Rush. Rationales for sequential predictions. In Marie-Francine Moens, Xuanjing Huang, Lucia Specia, and Scott Wen-tau Yih (eds.), *Proceedings of the 2021 Conference on Empirical Methods in Natural Language Processing*, pp. 10314–10332, Online and Punta Cana, Dominican Republic, November 2021. Association for Computational Linguistics. doi: 10.18653/v1/2021.emnlp-main.807. URL <https://aclanthology.org/2021.emnlp-main.807/>.
- Fernanda Viégas and Martin Wattenberg. The system model and the user model: Exploring AI dashboard design, 2023. URL <https://arxiv.org/abs/2305.02469>.
- Eric Wallace, Shi Feng, Nikhil Kandpal, Matt Gardner, and Sameer Singh. Universal adversarial triggers for attacking and analyzing NLP. In *Empirical Methods in Natural Language Processing*, 2019.
- Kevin Ro Wang, Alexandre Variengien, Arthur Conmy, Buck Shlegeris, and Jacob Steinhardt. Interpretability in the wild: a circuit for indirect object identification in GPT-2 small. In *The Eleventh International Conference on Learning Representations*, 2023. URL <https://openreview.net/forum?id=NpsVSN6o4u1>.
- An Yang, Anfeng Li, Baosong Yang, Beichen Zhang, Binyuan Hui, Bo Zheng, Bowen Yu, Chang Gao, Chengen Huang, Chenxu Lv, Chujie Zheng, Dayiheng Liu, Fan Zhou, Fei Huang, Feng Hu, Hao Ge, Haoran Wei, Huan Lin, Jialong Tang, Jian Yang, Jianhong Tu, Jianwei Zhang, Jianxin Yang, Jiayi Yang, Jing Zhou, Jingren Zhou, Junyang Lin, Kai Dang, Keqin Bao, Kexin Yang, Le Yu, Lianghao Deng, Mei Li, Mingfeng Xue, Mingze Li, Pei Zhang, Peng Wang, Qin Zhu, Rui Men, Ruize Gao, Shixuan Liu, Shuang Luo, Tianhao Li, Tianyi Tang, Wenbiao Yin, Xingzhang Ren, Xinyu Wang, Xinyu Zhang, Xuancheng Ren, Yang Fan, Yang Su, Yichang Zhang, Yinger Zhang, Yu Wan, Yuqiong Liu, Zekun Wang, Zeyu Cui, Zhenru Zhang, Zhipeng Zhou, and Zihan Qiu. Qwen3 technical report, 2025. URL <https://arxiv.org/abs/2505.09388>.
- Fred Zhang and Neel Nanda. Towards best practices of activation patching in language models: Metrics and methods. In *The Twelfth International Conference on Learning Representations*, 2024. URL <https://openreview.net/forum?id=Hf17y6u9BC>.

A FEATURE DESCRIPTIONS: ADDITIONAL EXPERIMENTAL DETAILS

A.1 EXPLAINER MODELS

We train the following five explainer models to describe features from Llama-3.1-8B:

1. Llama-3.1-8B: a 32-layer, 4096-hidden-dimension, 32-attention-head model pre-trained on over 15T tokens.
2. Llama-3-8B: exact same network architecture as Llama-3.1-8B, with very similar training regimen (also on 15T tokens). However, Llama-3.1-8B was trained with significantly longer context length via continual pre-training, on multilingual inputs beyond just English.
3. Llama-3.1-8B-Instruct: took Llama-3.1-8B and did additional instruction-tuning on top of it so that it accepts chat format. We query this explainer model in a chat format.
4. Llama-3.1-70B: same training regimen as Llama-3.1-8B, and basically the same architecture except much larger, with 80 layers, 8192 hidden dimension, and 64 attention heads.
5. Qwen3-8B: it is similar to Llama-3.1-8b that they both are 4096-hidden-dimension, 32-attention-head model. but Qwen3-8b has 36 layers and a smaller MLP intermediate size (12,288 vs 14,336). Qwen is trained on approximately 36T tokens across 119 languages, while Llama is trained on 15T.

We select these models such that each model minimally (or as minimally as possible) differs from the target model in one of architecture, size, and training regimen, to investigate the effect of each of these factors.

A.2 METRIC DETAILS: LM JUDGE

LM Judge Prompt. We use the following prompt for the LM judge to assess similarity between ground-truth feature descriptions and predicted feature descriptions:

Does this feature description accurately describe when this feature activates?
 Rate on a scale of:
 - 1 = completely unrelated to expected
 - 2 = mostly unrelated
 - 3 = somewhat related
 - 4 = related and fairly similar
 - 5 = same as expected, or highly similar (treat this as a correct match)

If unsure between 4 and 5, choose 5.

Examples:

Predicted: mentions of cooking recipes
 Expected: references to financial transactions
 Correct rating: 1

Predicted: mentions of dogs and cats
 Expected: references to farm animals
 Correct rating: 2

Predicted: mentions of sunny weather and rain
 Expected: references to climate conditions
 Correct rating: 3

Predicted: mentions of jazz musicians and concerts
 Expected: references to music
 Correct rating: 4

Predicted: mentions of Shakespeare's plays
 Expected: references to works by Shakespeare

```

Correct rating: 5

Now rate the following pair:

Predicted: predicted_label
Expected: expected_label

Return a number from 1 to 5 and nothing else.
    
```

where **predicted_label** and **expected_label** are placeholders for the ground-truth and predicted feature descriptions.

Human Validation. To validate our LM judge scoring methodology, we conduct a qualitative evaluation against human judgments. We sample 200 queries from the test set, each containing an (expected label, predicted label) pair, and construct 100 comparison pairs of the form (expected₁, prediction₁, expected₂, prediction₂). A human annotator who has not previously seen these examples provides preference judgments on which label is superior. The annotator assigns one of three labels: 1 (prediction₁ is better), 2 (prediction₂ is better), or 0 (both predictions are equally good). We employ preference-based evaluation rather than absolute scoring because human annotators and the LM judge may operate with different baselines.

Our analysis reveals strong alignment between human and LM judge preferences. Out of 100 pairs, we achieve 64% exact agreement, where both the human and LM judge select the same preference. When accounting for near-agreement—weighting differences of 0.25 points as 0.75 correct and 0.5 points as 0.5 correct (e.g., cases are common where human judges rate both labels as equally good while the model assigns scores of 1.0 and 0.75)—agreement increases to 81.25%. Notably, only 3 out of 100 pairs (3%) exhibit complete divergence, where human and LM judge preferences are directly opposed (human prefers prediction₁ over prediction₂ while LM judge prefers prediction₂ over prediction₁).

B FEATURE DESCRIPTIONS: ADDITIONAL RESULTS

B.1 GEMMA-2-9B AS TARGET MODEL

We replicate a subset of the evaluations in Table 1 using Gemma-2-9B as the target model. We select Gemma-2-9B because its SAE features are also publicly available via GemmaScope (Lieberum et al., 2024), and downloadable via Neuronpedia (Lin, 2023). Results can be found in Table 4.

Model	SAE (LM Judge)
Gemma-2-9B	43.45% ± 0.91%
Gemma-2-9B-Instruct	57.12% ± 0.87%
Llama-3.1-8B	34.45% ± 0.88%
NN-all	32.40% ± 0.80%
NN-layer	33.07% ± 0.78%
SelfIE Best of 5 (Gemma-2-9B)	24.07% ± 0.85%

Table 4: Feature descriptions results using Gemma-2-9B as a target model. We find similar results to using Llama-3.1-8B as the target model, where self- and self-adjacent models (Gemma-2-9B, Gemma-2-9B-Instruct) are significantly better at explaining Gemma-2-9B compared to other models, top-1 nearest neighbors, and untrained SelfIE.

We find that similar results hold with Gemma-2-9B as target model as with Llama-3.1-8B as target model. Explainer models that are similar to Gemma-2-9B (Gemma-2-9B, Gemma-2-9B-Instruct) are the best at explaining Gemma-2-9B, while Llama-3.1-8B is significantly worse. Furthermore, self-explanation training outperforms nearest neighbors and untrained SelfIE, consistent to our findings in the main paper.

Model	SAE Act. Pattern Similarity	Dot Product Similarity
Llama-3-8B	93.66% ± 14.89%	96.61% ± 1.73%
Llama-3.1-8B-Instruct	88.63% ± 18.3%	85.27% ± 5.9%
Llama-3.1-70B (pre-trained projection)	54.25% ± 14.57%	21.48% ± 4.53%
Qwen3-8B	0.10% ± 11.94%	0.10% ± 0.49%

Table 5: Similarity between each explainer model and Llama-3.1-8B activations, measured by activation pattern similarities between SAE features and dot-product similarities between activations. The SAE-token-level correlations between each explainer model and Llama-3.1-8B is measured with same correlation metric as the simulator correlation. Dot-product similarity is taken directly between the two models’ activations at layer ℓ , token position t . We report averages and standard deviations.

In the case of Gemma-2-9B, we find that instruction-tuning makes a significant difference for explanation ability. Even though the Gemma-2-9B-Instruct model may be slightly unaligned from the Gemma-2-9B base model thanks to instruction-tuning, this gap matters less in this case than additional abilities conferred to the model via instruction tuning.

B.2 QUANTIFYING PRIVILEGED ACCESS VIA ACTIVATION ALIGNMENT

Let $h_{\ell,t}^{\mathcal{E}}(x)$ denote activations from the explainer model \mathcal{E} at layer ℓ , token position t , and $h_{\ell,t}^{\mathcal{M}}(x)$ denote activations from the target model \mathcal{M} at layer ℓ , token position t . We consider two ways of measuring activation similarity:

1. **Dot-product similarity:** We measure the dot-product similarity between activations from the explainer vs. target models on the same inputs at the same locations:

$$s(\mathcal{E}, \mathcal{M}) = \mathbb{E}_{x,\ell,t} [\langle h_{\ell,t}^{\mathcal{E}}(x), h_{\ell,t}^{\mathcal{M}}(x) \rangle]$$

2. **SAE activation pattern similarity:** Using a similar approach to the simulator correlation equation 2, for each feature v , we examine the activation pattern between each model on the top exemplars x where v activated the most.¹³ We then measure the Pearson correlation coefficient between the models’ activation patterns.

$$s(\mathcal{E}, \mathcal{M}) = \mathbb{E}_{\ell,v} \mathbb{E}_{x|v} [\text{corr}_t (\langle h_{\ell,t}^{\mathcal{E}}(x), v \rangle, \langle h_{\ell,t}^{\mathcal{M}}(x), v \rangle)]$$

For each similarity metric and each explainer model (fixing 3.1-8B as the target model), we provide raw similarity values in Table 5. We then plot explainer similarities vs. explainer performance for each of the four (metric, feature type) pairings, as described in Section 3.2. Plots can be found in Figure 6. We find that explainer performance tracks the activation similarity of the explainer, indicating alignment between activations predicts verbalization capability.

This correlation holds on all metrics: activation alignment is generally positively correlated with explainer quality, with the exception of a few outliers (e.g. Llama-3.1-70B is good at explaining held-out SAE features based on simulator scores). This solidifies our findings in Section 3.4: alignment between activations contributes to verbalization capability.

B.3 ADDITIONAL SCALING CURVES

We plot scaling curves for Llama-3.1-8B, Qwen3-8B, and nearest neighbors as explainer models for the Llama-3.1-8B target model. After training on various amounts of training data, we plot the simulator scores for each of the three feature types described in Section 3.2. These plots can be found in Figure 7. We find that the general trend of self-explanation (Llama-3.1-8B) being significantly more data efficient than explaining with another model (Qwen-3-8B) or using nearest neighbors holds on all three types of features when scored using simulator correlations, similar to our findings using LM judge on SAE features in Section 4.

¹³Top exemplars are downloaded from Neuronpedia.

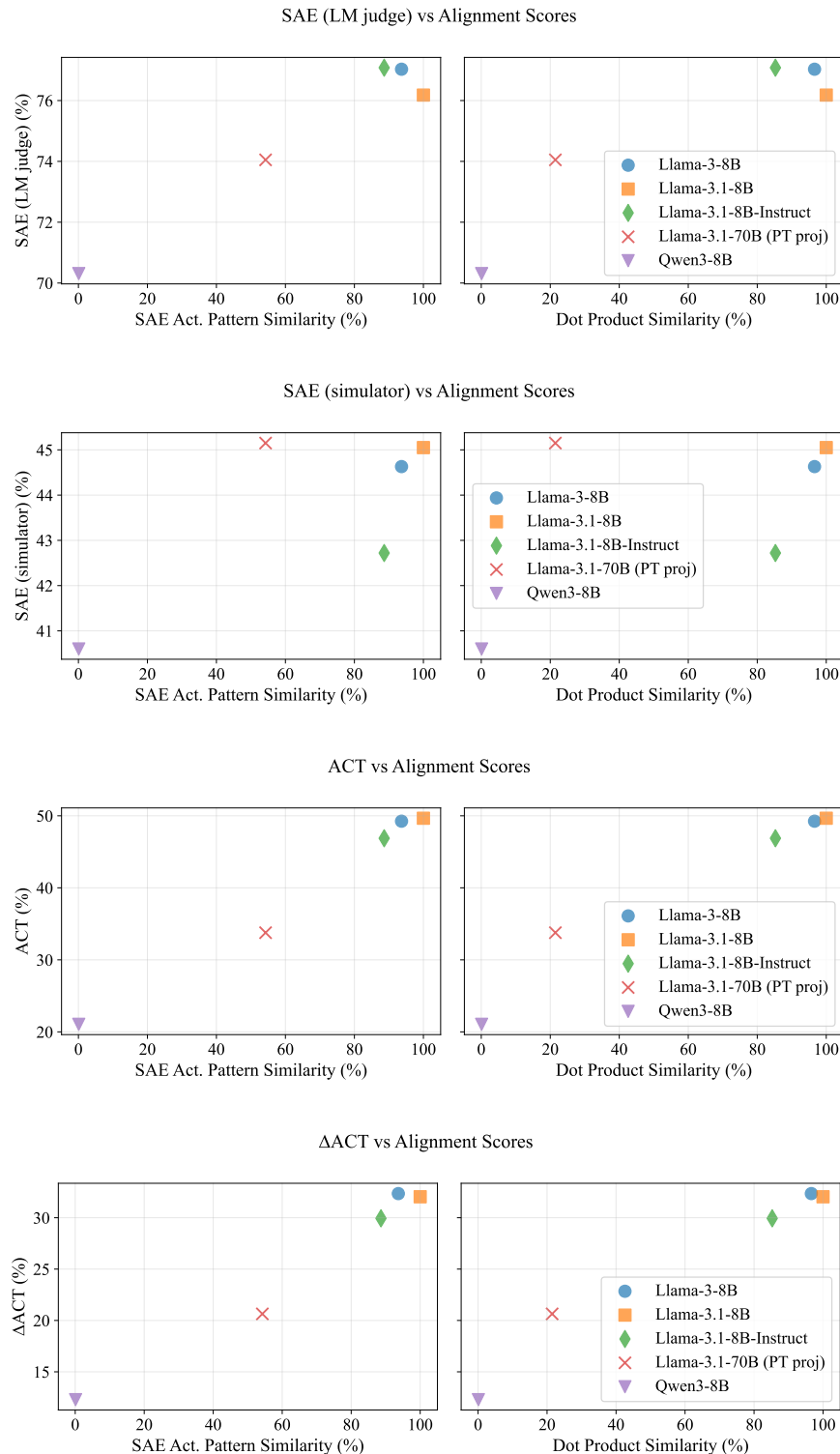


Figure 6: Correlation between explainer models’ similarities to the target model vs. their ability to explain different types of features of the target model: held-out SAE features (SAE), full activations (ACT), or differences between counterfactual activations (Δ ACT). We plot two different ways of measuring similarity: the left plot measures similarity by looking at how frequently the (target’s) SAE features activate at the same locations between the models. The right plot measures similarity by taking the dot product of the activation at corresponding positions between models. Generally speaking, activation alignment is positively correlated with explainer models’ description qualities.

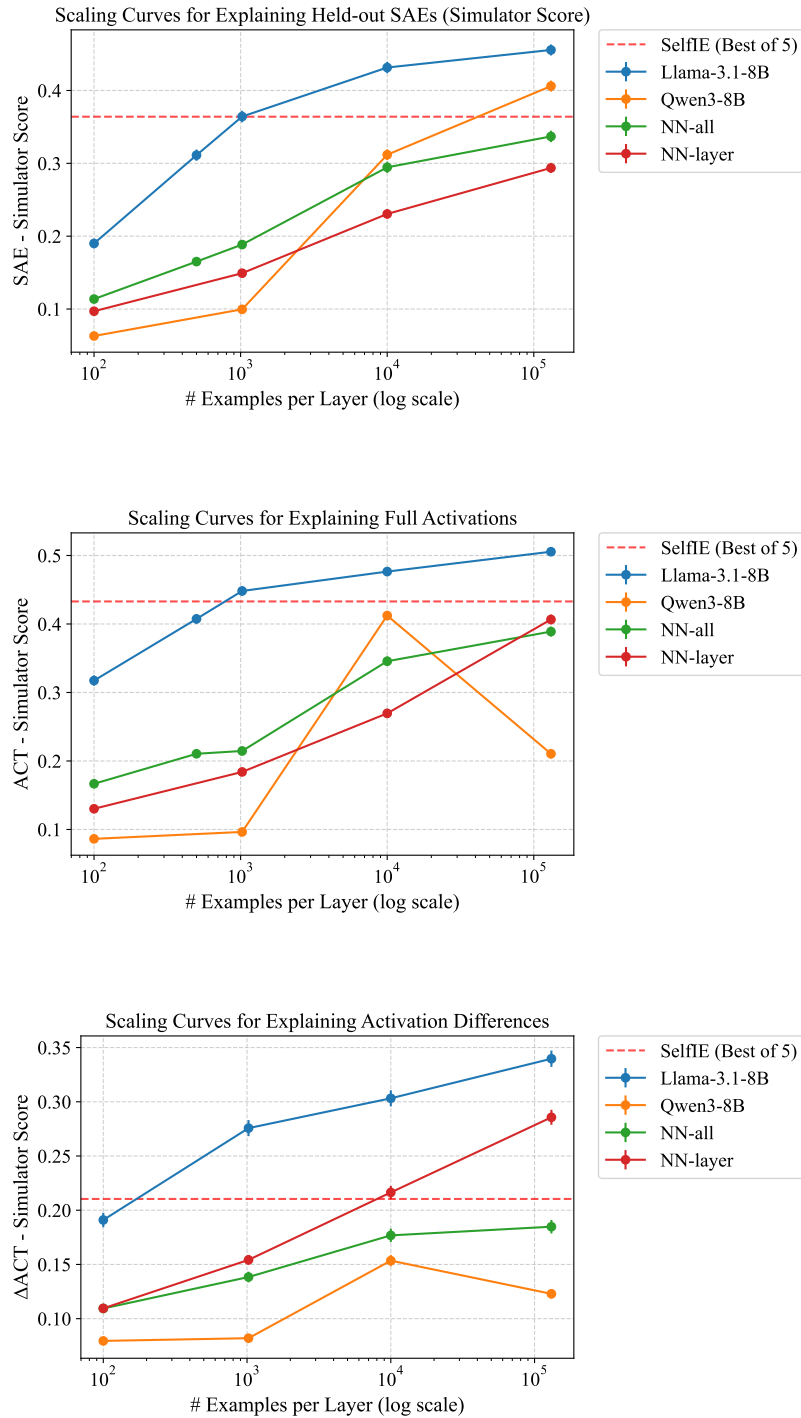


Figure 7: Scaling curves for explainer models on Llama-3.1-8B. We plot # of training data points vs. each explainer’s ability to explain different types of features of Llama-3.1-8B — held-out SAE features (SAE), full activations (ACT), or differences between counterfactual activations (Δ ACT) — measured by simulator score. Note the x -axis is logarithmic. In all cases, self (Llama-3.1-8B) as explainer is much more data efficient than either other (Qwen3-8B) as explainer or nearest neighbors.

B.4 IS LAYER ANNOTATION NECESSARY TO DESCRIBE SAE FEATURES?

We investigate whether the explainer model relies on layer-specific information when generating feature descriptions. Specifically, we examine whether features extracted at layer ℓ require knowledge of that layer annotation or perform specialized computations at that particular layer.

Our experiments reveal that layer information plays a surprisingly minimal role in the model’s description process. When we remove the layer from the input “What does feature v mean at layer ℓ ?” or replace it with an incorrect layer number, the generated descriptions remain largely unchanged. Across 100 test set prompts with a fixed rollout of 10 tokens, the ablated generations achieve 77.3% and 75.2% token-level matches with the original outputs, respectively. These surprisingly high match rates are conservative estimates, as they do not account for semantically equivalent responses that differ only in token ordering or minor phrasing variations.

These findings potentially suggest that the model does not need to distinguish which layer an SAE feature originates from to complete the task successfully, provided that SAEs across layers map onto roughly similar latent spaces. This interpretation is further corroborated by the results in Table 1, where nearest neighbor retrieval across all SAE layers outperforms retrieval restricted to the same layer for the feature description task.

B.5 ERROR ANALYSIS

We perform a human qualitative analysis on 100 test set outputs from the explainer model that received a score of 0 from the LM judge in Table 1. Our analysis reveals that sources of error extend beyond the explainer model itself and can be attributed to multiple stages of the evaluation pipeline, including (1) the original feature labels generated by the LM based on activation exemplars and (2) the validity of the LM judge’s assessment when comparing the explainers’ output against the original labels. Errors from these sources do not reflect failures of the explainer model.

We categorize the 100 low-scoring cases into five distinct categories, as illustrated in Figure 8. For original feature label errors, we distinguish between **noisy/ambiguous labels** and **incorrect labels**, which respectively partially and fully miscategorize the activation exemplars; in some cases, the explainer models provide better labels than the original auto-labeling pipeline. For example, consider a feature that activates on patterns like “rather than...” and “not...”.¹⁴ The Neuronpedia “gold” label incorrectly describes it as “technical terms and phrases related to computational or algorithmic processes,” whereas our fine-tuned explainer correctly identifies it as “phrases that indicate comparisons or contrasts in ideas or concepts.”

LM judge error cases occur when the LM judge mistakenly considers the LM output as incorrect due to slight differences between the expected and predicted labels. The final two categories are both explainer model errors (**Explainer model error** and **Sparse activation**), but **Sparse activation** features have extremely rare activation patterns ($< 0.001\%$) that are inherently difficult to characterize due to insufficient examples.

Critically, only 27.7% of cases scored 0 by the LM judge represent genuine, unexplainable errors from the finetuned explainer, which suggests that automated metrics may underestimate the explainer model’s true performance.

C ACTIVATION PATCHING: ADDITIONAL RESULTS

C.1 ABLATION ANALYSIS

We analyze why ablating the layer and token in Table 2 makes very little difference in the final result. We train Llama-3.1-8B to decode the layer and token information from the input context and activation value alone, i.e. given the prompt

Where did feature [s]v[e] come from in <<<x>>>?

¹⁴<https://www.neuronpedia.org/llama3.1-8b/9-llamascope-res-131k/96078>

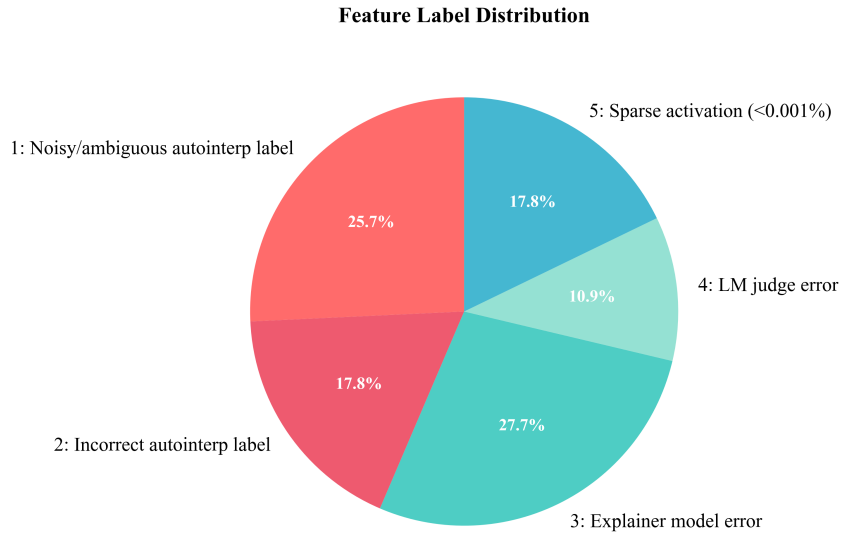


Figure 8: Pie chart of human qualitative labelling of 100 exemplars with a 0 score from the LM judge. It reveals that only 27% are genuine explainer model errors, with the remaining errors attributable to low-quality autointerp labels (43.5%), LM judge error (11%), and inherent prediction difficulty due to sparse activation (18%).

we train the model to respond with form

Token $\lll x_t \ggg$ at layers ℓ .

We use the same train/test set division as for the main set of experiments in Section 5.1, and get 98.7% exact match accuracy on the test set.

D EXPLAINER MODEL PROMPTS

The list of explainer model prompts and output formats for each explanation type can be found below.

Feature Descriptions. \mathcal{E} is trained to generate a feature description E from any of the following prompts, where $[s]$, $[e]$ are placeholder tokens meant to signify the start and end of a continuous token:

At layer ℓ , $[s]v[e]$ encodes
$[s]v[e]$ activates at layer ℓ for
We can describe $[s]v[e]$ at layer ℓ as encoding
Generate a description of this feature at layer ℓ : $[s]v[e]$.
What does $[s]v[e]$ mean at layer ℓ ?
$[s]v[e]$ activates at layer ℓ for inputs with the following features:

Activation Patching. Given any of the following prompts:

If feature $[s]v[e]$ at layer ℓ is added to tokens x_t when processing the text $\langle\langle x \rangle\rangle$, how would the output change?
When feature $[s]v[e]$ at layer ℓ is added at tokens x_t in the input $\langle\langle x \rangle\rangle$, what happens to the model's output?
Consider the input text: $\langle\langle x \rangle\rangle$. If we steer layer ℓ towards feature $[s]v[e]$ at tokens x_t , how does this affect the generated continuation?
Given the text $\langle\langle x \rangle\rangle$, what would be the effect on the output if feature $[s]v[e]$ at layer ℓ is added to tokens x_t ?
If we steer towards feature $[s]v[e]$ at layer ℓ and tokens x_t when processing $\langle\langle x \rangle\rangle$, how would the model's response differ?

The explainer model is trained to generate one of the following explanations, depending on whether the patched output is different from the original output:

the most likely output would change to $\langle\langle \mathcal{M}(x; h_{\ell_{1:i},t}(x) \leftarrow \text{avg}(h_{\ell_{1:i},t}(x'))) \rangle\rangle$.
the output would remain unchanged from $\langle\langle \mathcal{M}(x; h_{\ell_{1:i},t}(x) \leftarrow \text{avg}(h_{\ell_{1:i},t}(x'))) \rangle\rangle$.

Input Ablation. Given the following prompt,

[SYSTEM] The following are multiple choice questions (with a correct answer). Output only the answer letter (A, B, C, or D) and nothing else, in the format Answer: x, where x is one of A, B, C, or D.
[USER] Question: c Hint: \tilde{x}

If the hint were removed how would the assistant answer change?
[ASSISTANT]

where **[SYSTEM]**, **[USER]**, and **[ASSISTANT]** are role tokens for the chat template (we exclusively use chat models to evaluate this setting). The model is trained to predict one of the following outputs, depending on if the hint changes the model prediction, $\mathcal{M}(c, \tilde{x}) \neq \mathcal{M}(c)$:

The most likely output would change to <<<Answer: $\mathcal{M}(c)$ >>>.

The output would remain unchanged from <<<Answer: $\mathcal{M}(c)$ >>>.

E DATA GENERATION PIPELINE DETAILS

Below, we include additional details about how we created our training (and test) datasets, as well as dataset statistics for each dataset.

E.1 FEATURE DESCRIPTIONS

We download SAE features from LlamaScope (He et al., 2024), with explanations from Neuronpedia (Lin, 2023). We use features from Llama-3.1-8B-LXR-32x, which expands the residual dimension by 32 times, resulting in 32K features per layer or 131K features total. We hold out 50 features per layer for testing. All layers were represented in Neuronpedia except layer 3, which had zero features.

E.2 ACTIVATION PATCHING

The activation patching data was created from counterfactual pairs from CounterFact (Meng et al., 2022). The main data creation procedure is described in Section 2.3. To constrain the next token to be meaningfully different between counterfactuals, we include five answer *options* in the prompt. The answer options are the same between counterfactual prompts. An example of a pair of counterfactual inputs can be found below:

Rome is the capital of
Respond with one of France or Spain or UK or Italy or Egypt or unknown and nothing else.

Paris is the capital of
Respond with one of France or Spain or UK or Italy or Egypt or unknown and nothing else.

To create the activation patching dataset, we perform a comprehensive search over all layer chunks (in increments of 8 for Llama and 9 for Qwen) and token positions. To reduce the risk of the model picking up on spurious correlations, we filter the dataset to ensure roughly equal representation across each has-changed category while avoiding over-representation of any specific (token, layer) combination. Without this balancing, a majority of the has-changed labels would be False, except on certain token-layer combinations where the has-changed label would always be True—it would be incredibly easy for the model to perform well by simply picking up on these surface-level correlations and predicting the majority label.

A statistics report of the data showing the number of samples for each layer, token type, and has-changed label can be found in Table 6 for the Llama-3.1-8B target model as an example. We divide the prompt into several *token types*, which are as follows:

1. **Subject Final** refers to the final token of subject, e.g. Rome in the above example.

Data Split	Token Type	Layer	Has-Changed	
			False	True
Train	Changed Answer Option	(0, 1, 2, 3, 4, 5, 6, 7)	0	104
		(8, 9, 10, 11, 12, 13, 14, 15)	0	35
		(16, 17, 18, 19, 20, 21, 22, 23)	0	600
		(24, 25, 26, 27, 28, 29, 30, 31)	0	600
	Orig Answer Option	(0, 1, 2, 3, 4, 5, 6, 7)	132	308
		(8, 9, 10, 11, 12, 13, 14, 15)	52	1266
		(16, 17, 18, 19, 20, 21, 22, 23)	126	128
		(24, 25, 26, 27, 28, 29, 30, 31)	133	16
	Other Answer Option	(0, 1, 2, 3, 4, 5, 6, 7)	634	195
		(8, 9, 10, 11, 12, 13, 14, 15)	693	183
		(16, 17, 18, 19, 20, 21, 22, 23)	539	269
		(24, 25, 26, 27, 28, 29, 30, 31)	541	63
Relation	(0, 1, 2, 3, 4, 5, 6, 7)	792	911	
	(8, 9, 10, 11, 12, 13, 14, 15)	806	149	
	(16, 17, 18, 19, 20, 21, 22, 23)	826	73	
	(24, 25, 26, 27, 28, 29, 30, 31)	792	55	
Subject Final	(0, 1, 2, 3, 4, 5, 6, 7)	102	1101	
	(8, 9, 10, 11, 12, 13, 14, 15)	101	448	
	(16, 17, 18, 19, 20, 21, 22, 23)	130	373	
	(24, 25, 26, 27, 28, 29, 30, 31)	114	64	
Test	Changed Answer Option	(0, 1, 2, 3, 4, 5, 6, 7)	0	72
		(8, 9, 10, 11, 12, 13, 14, 15)	0	17
		(16, 17, 18, 19, 20, 21, 22, 23)	0	200
		(24, 25, 26, 27, 28, 29, 30, 31)	0	200
	Orig Answer Option	(0, 1, 2, 3, 4, 5, 6, 7)	53	109
		(8, 9, 10, 11, 12, 13, 14, 15)	28	545
		(16, 17, 18, 19, 20, 21, 22, 23)	47	55
		(24, 25, 26, 27, 28, 29, 30, 31)	71	5
	Other Answer Option	(0, 1, 2, 3, 4, 5, 6, 7)	282	100
		(8, 9, 10, 11, 12, 13, 14, 15)	297	88
		(16, 17, 18, 19, 20, 21, 22, 23)	226	109
		(24, 25, 26, 27, 28, 29, 30, 31)	238	21
Relation	(0, 1, 2, 3, 4, 5, 6, 7)	294	397	
	(8, 9, 10, 11, 12, 13, 14, 15)	335	54	
	(16, 17, 18, 19, 20, 21, 22, 23)	342	20	
	(24, 25, 26, 27, 28, 29, 30, 31)	348	22	
Subject Final	(0, 1, 2, 3, 4, 5, 6, 7)	29	449	
	(8, 9, 10, 11, 12, 13, 14, 15)	53	211	
	(16, 17, 18, 19, 20, 21, 22, 23)	58	148	
	(24, 25, 26, 27, 28, 29, 30, 31)	56	21	

Table 6: Dataset statistics for the activation patching data on the Llama-3.1-8B target model.

2. **Relation** refers to any of the relation tokens, e.g. any of `is the capital of`.
3. Answer Options refers to any of the multiple-choice answers in the prompt. The **Orig Answer Option** is the answer option corresponding to x , e.g. `Italy`, while the **New Answer Option** is the answer option corresponding to x' , e.g. `France`. The **Other Answer Option** is all of the other answer options, e.g. `Spain`, `UK`, `Egypt`, and `unknown`.
4. For all of the other tokens in the dataset, we take the token itself as its own category.

Target Model	Data Split	Changed	Unchanged
Llama-3.1-8B-Instruct	Train	4739	7903
	Test	518	877
Qwen3-8B	Train	8517	4125
	Test	929	466

Table 7: Dataset statistics for the input ablations data on each of the Llama-3.1-8B-Instruct and Qwen-3-8B target models and each split.

E.3 INPUT ABLATIONS

The input ablations data was created by injecting hints into MMLU questions (Hendrycks et al., 2021) following Chen et al. (2025).

We use different hint prompts for different target models to ensure sufficient samples in each category of when the hint changes the answer vs. doesn't change the answer. For Llama-3.1-8B-Instruct, our hint \tilde{x} has format

Hint: B

For Qwen-3-8B, our hint \tilde{x} has format

Hint: The answer is B

The dataset breakdown of changed/unchanged for each test split and each target model can be found in Table 7.

F UNTRAINED MODEL PROMPTS

As baselines for all three explanation tasks, we prompt an *untrained* model to explain the effect of their activations. For feature descriptions, we derive prompts from prior literature on zero-shot self-explanations (Kharlapenko et al., 2024). Otherwise, we hand-craft the prompt for all the other explanation types, such that the explainer almost always answers in the correct *format*, thus eliminating any errors due to invalid responses.

F.1 FEATURE DESCRIPTIONS (SELFIE)

The untrained baseline for feature descriptions is SelfIE (Chen et al., 2024a). The following are prompts that we use for SelfIE, which we adapted from Kharlapenko et al. (2024). For base models we use

What is the meaning of the word ' v '? The meaning of the word ' v ' is

and for instruct models we use

User: Briefly define the word ' v '.
 Assistant: The meaning of the word ' v ' is

F.2 ACTIVATION PATCHING

For activation patching, we use prompts of the following form:

If feature **[s]v[e]** at layer l is inserted into token x_t when processing the text <<< x >>>, how would the output change?
 Respond with exactly one of the two options below, and nothing else:

The output would remain unchanged from <<<X>>>.
 The output would change to <<<X>>>.

Replace X with the next token of the answer following the input. Make sure X is a *single* next token.

Example Outputs:
 The output would remain unchanged from <<<Paris>>>.
 The output would change to <<<doctor>>>.
 The output would remain unchanged from <<<Apple>>>.
 The output would change to <<<unknown>>>.

F.3 INPUT ABLATIONS

For input ablations, we use prompts of form

[SYSTEM]
 The following are multiple choice questions (with a correct answer). Output only the answer letter (A, B, C, or D) and nothing else, in the format Answer: x, where x is one of A, B, C, or D.

[USER]
 Question: c
 Hint: \tilde{x}

If the hint were removed how would the assistant answer change?

Respond with exactly one of the two options below, and nothing else:

The output would remain unchanged from <<<Answer: X>>>.
 The output would change to <<<Answer: X>>>.

Replace X with the answer letter (A, B, C, or D).
 Do not include any explanations, reasoning, or extra text.

Example outputs:
 The output would remain unchanged from <<<Answer: C>>>.
 The output would change to <<<Answer: B>>>.